REVIEWS

Recent advances in auto exhaust catalysis

Parthasarathi Bera[1] AND M. S. Hegde[2]

Abstract | In last 30 years innovative research in the area of auto exhaust catalysis is being developed and CeO_2 has been found to play a major role in this area due to its unique redox properties. In this review, auto exhaust emission and its impact on earth's environment, global concern and recent advances in science and technology in automotive exhaust catalysis have been documented. A new preparative method of dispersing metal ions by solution combustion technique over CeO_2 and TiO_2 resulting mainly $Ce_{1-x}M_xO_{2-\delta}$, $Ti_{1-x}M_xO_{2-\delta}$ and $Ce_{1-x-y}Ti_xM_yO_{2-\delta}$ (M = Pd, Rh and Pt) catalysts, structure of these materials, their catalytic properties towards auto exhaust catalysis, structure–property relation and mechanism of catalytic reactions are accounted here. In these materials, metal ions are incorporated into substrate matrix to a certain limit in the solid solution form and we have established a new direction in heterogeneous catalysis by turning to the concept of dispersed metal ions as catalytically active sites from the conventionally nurtured idea of metal particles as active centers for catalysis.

1. Introduction

The industrial development in the world is mainly accompanied by the consumption of fossil fuels such as coal, natural gas and oil. Most of the fossil fuels constitute carbon, nitrogen, hydrogen and to some extent sulfur containing compounds. The energy stored in the fossil fuels, biomass, industrial and domestic waste is released mostly by complete as well as partial combustion of these constituents leading to emission of nitrogen oxides (NO_x), carbon monoxide (CO), sulfur oxides (SO_x), NH_3 and unburned hydrocarbons (HC) to the atmosphere which cause environmental pollution. These pollutants are emitted everyday with the effluents produced by mobile and stationary sources. The mobile sources of emission include automotive emissions and emissions from aeroplanes, whereas the stationary sources are industrial processes, power plants, combustion of waste and biomass and domestic burning.

Practically, in the last decade, mammoth increase in the number of road and air traffics as well as industrial activities especially around the thickly populated mega cities in the developed as well as developing countries add a substantial contribution to environmental pollution and hence, this whole man made situation causes a big threat to the living being on earth. Therefore, it is necessary to control these pollutants for sake of our environment. There are several technologies for controlling exhaust emissions. Among available technologies one of the best ways of controlling exhaust emission could be to reduce or convert these pollutant gases by using catalyst at the source itself. The conversion of these environmentally unacceptable gases to N_2, CO_2 and H_2O using catalysts is a challenging task. Therefore, environmental catalysis or exhaust catalysis has been growing as a new and broad area of research in heterogeneous catalysis in the last three decades. However, environmental

[1]Surface Engineering Division, National Aerospace Laboratories, Bangalore 560017, India
[2]Solid State and Structural Chemistry Unit, Indian Institute of Science, Bangalore 560012, India
mshegde@sscu.iisc.ernet.in

catalysis related to auto exhaust has received much more attention as exhaust from automobiles has significant contribution to the global environment pollution. Extensive studies on the scientific research and technological development in this area has been carried out over the last several years. A number of reviews and articles regarding various aspects of exhaust catalysis have been published to update the status of catalytic science and technological development in this area from time to time.[1–28] Kašpar and coworkers have enlighted the scenario of automotive catalytic converters for the 21st century.[23] An assessment of the developments in automotive catalysis and its future directions as we enter 21st century have been briefed by Twigg.[29–32] In a recent comprehensive review, Roy and Baiker have presented several aspects of NO$_x$ storage and reduction (NSR) catalysis where they have discussed mechanism of NSR catalysts, role played by noble metals, storage components and support oxides.[33] Roy et al. has briefed NO$_x$ abatement catalysis in a recent review where they have provided updated information about several NO$_x$ removal techniques such as photocatalytic decomposition and reduction of NO$_x$, selective catalytic reduction (SCR) of NO and NSR catalysis.[34] Keeping several type of catalysts for auto exhaust catalysis in our mind, new generation catalysts have been developed in our laboratory in last one decade in order to understand the metal ion–reducible support interaction, relation between structure and oxygen storage capacity (OSC), synergistic effect and catalytic activity.[35] In this review, we would account, the global concern on auto exhaust emission, current status as well as recent developments in advanced materials for auto exhaust catalysis. Finally, future direction of auto exhaust catalysis in the 21st century view point would also be discussed.

2. Formation of pollutants and their adverse effects

The atmosphere is a chemically complex and dynamic system that interacts significantly with the land, oceans and ecosystems. The atmosphere is the recipient of a vast array of chemical compounds emitted by natural processes and in recent times, increasingly emitted by human activities. The oxidation of this wide variety of chemical compounds is a key process proceeding in our oxygen-rich atmosphere. Most trace gases emitted into the atmosphere are removed by oxidation reactions involving ozone and the hydroxyl free radical. Hence, oxidation reactions are sometimes referred to as nature's atmospheric 'cleansing' process. Without an efficient oxidation process, levels of many emitted gases could rise to

such high levels, relative to natural composition level, that they would radically change the chemical nature of our atmosphere and biosphere. On the other hand, the industrial revolution in the past 150 years, together with increased biomass burning associated with human land use, has led to significant increases since preindustrial times in the global emissions of NO$_x$, SO$_x$, CO and HCs that varies from country to country.[36] Also, the observed temperature increase of 0.6 ± 0.2 °C in this time period should have led to increases in lower level atmospheric H$_2$O and possibly changes in global cloud cover. Therefore, all these human related activities have affected O$_3$ and OH concentrations of the natural (preindustrial) state, thereby disturbing oxidation processes that occur in the nature and hence, abrupt changes in our environment have augmented.[37]

Exhaust gas or flue gas is emitted as a result of the combustion of fuels such as natural gas, gasoline (petrol), diesel, fuel oil or coal. It is discharged into the atmosphere through an exhaust pipe, flue gas stack or propelling nozzle. The principal pollutants present in auto exhaust emission gases are NO$_x$, CO and unburned HC. Other gases like H$_2$, N$_2$O, NH$_3$, CO$_2$, and SO$_x$ are also present to some extent. In case of diesel engine, exhaust, however, contains particulate matters (PM) composed of solid dry carbon or soot and unburned liquid fuel and lubricating oil called the soluble organic fraction (SOF) or volatile organic fraction (VOF). Furthermore, the gaseous exhaust from diesel engine contains significant amounts of SO$_2$. Over most oxidation catalysts, SO$_2$ would be converted to SO$_3$ that eventually turned into H$_2$SO$_4$. This unfavorable secondary emission obviously contributes to the total particulates.

Automobile engine exhaust gas composition is a complex mixture that depends on variety of factors such as type of engine, driving condition, vehicle speed and so on. There are two types of engines such as gasoline powered engine and diesel powered engine. Generally, gasoline engines are referred to as internal combustion engine (ICE) where initiation of the combustion process of air–fuel mixture is ignited within the combustion chamber and the ignition is done either by spark ignition (SI) or compression ignition (CI). Gasoline powered two-stroke and four-stroke engines are such kind of ICEs where combustion is intermittent. A two-stroke engine completes the thermodynamic cycle in two movements of the piston, whereas engines based on the four-stroke have one power stroke for every four strokes (up–down–up–down) and employ spark plug ignition. A four-stroke spark-ignition engine is also called Otto cycle engine. The two-stroke engine

Table 1: Typical exhaust gas composition of a gasoline powered spark ignition internal combustion engine.

Gases	Vol. (%)
N_2	71.0
CO_2	18.0
H_2O	9.2
O_2 and noble gases	0.7
Pollutants	
(a) CO	0.85
(b) NO_x	0.08
(c) Unburned HCs	0.05
(d) Particulate matters	0.005
Others	0.115
Total	100

Table 2: Estimated global sources of NO_x.

Sources	NO_x (10^9 kg N yr^{-1})	Percentage (%)
I. Human sources		
Stationary	13	24
Mobile	8	15
Biomass burning	12 (4–24)	22
Agriculture	5 (1–10)	9
II. Normal sources		
Soils	8 (4–16)	15
Oceans	<1	-
Lightening	8 (2–20)	15
Others	~0.5	-
Total	55 (25–100)	100

was popular throughout most of the 20th century in motorcycles and some cars. This was due to their simple design leading to low cost and higher power-to-weight ratios. Its overall light weight and light-weight spinning parts give important operational and even safety advantages. Most designs used total-loss lubrication with the oil being burnt in the combustion chamber causing visible and other pollution. This is the major reason for two-stroke engines being gradually replaced with four-stroke engines in most applications. In four-stroke engines, combustion occurs rapidly with more or less constant volume. They are used in cars, larger boats, some motorcycles and many light aircrafts. They are generally quieter, more efficient and larger than their two-stroke counterparts. On the other hand, diesel fueled engines are compression-ignition engine (CIE) where the heat generated from the compression is enough to initiate the combustion process. Most truck and automotive diesel engines use a cycle reminiscent of a four-stroke cycle, but with a compression heating ignition system, rather than needing a separate ignition system. This variation is called the diesel cycle. In the diesel cycle, diesel fuel is injected directly into the cylinder so that combustion occurs at constant pressure as the piston moves, rather than with the four-stroke with the piston essentially stationary. However, amount of NO_x produced from diesel engine is less due to its cooler combustion nature compared with gasoline engine. Typical exhaust gas composition of a gasoline powered spark ignition internal combustion engine is given in Table 1.[26]

The main atmospheric oxides of nitrogen include nitric oxide (NO), nitrogen dioxide (NO_2) and nitrous oxide (N_2O). Collectively, NO and NO_2 are commonly referred to as NO_x. For more than a century, atmospheric levels of nitrogen oxides have been increasing steadily. While a significant amount of this increase has been due to human activity, natural sources also make important contributions to the overall NO_x levels. Relative contributions

of global NO_x emission from different sources are given in Table 2.[38] But it varies from country to country and year to year. Table 3 shows a typical amount of NO_x emission from various sources in US for the year 2005.[39] The exhaust hydrocarbons are a mixture of paraffins, olefins and aromatics ranging from C_1 to C_8. Various aldehydes, alcohols, esters and ketones are also found in exhaust gases at concentrations upto several hundred parts per million. Several volatile organic compounds (VOC) are also emitted from a variety of stationary sources such as solvent evaporation, organic chemical manufacturing and catalyst regeneration. Flue gas from waste incinerators is composed of NO_x, CO, HCl, HF and SO_2. In general, auto exhaust gas pollutant concentration depends mainly on air to fuel (A/F) ratios. A/F is generally defined as:

$$A/F = \frac{\text{mass of air consumed by the engine}}{\text{mass of fuel consumed by the engine}}.$$

The engine out exhaust gas composition is also commonly classified in terms of λ and it is defined as:

$$\lambda = \frac{\text{actual engine A/F}}{\text{stoichiometric engine A/F}}.$$

For gasoline engines, the stoichiometric value of A/F ratio occurs at 14.7. At this stoichiometric point, amount of oxidants is equal to that of reducing agents. If the A/F ratio is below this value, then it is called fuel-rich condition and the exhaust gas contains more reducing agents like CO and HC. On the other hand, if A/F ratio exceeds this value, then it is called fuel-lean condition and the exhaust gas contains more oxidizing agents like NO and O_2.

Pollutant gases emitted from exhausts have harmful effects on earth's atmosphere, ecological system and also on human health. NO_x plays a major role in the photochemistry of troposphere and stratosphere, where it catalyzes the formation of ground level ozone and ozone layer depletion, respectively. The troposphere is the lowest layer

Table 3: Amount of NO_x emission from various sources in US for the year 2005.

Source sectors	Total emission (Ton)
On road vehicles	6,491,821
Non road equipment	4,162,872
Electricity generation	3,783,659
Fossil fuel combustion	2,384,297
Industrial processes	1,163,635
Waste disposal	155,415
Fires	94,372
Residential wood combustion	38,324
Solvent use	6,400
Fertilizer and livestock	2,098
Miscellaneous	3,644

of the atmosphere, extending from the ground to roughly 10–15 km altitude, whereas the stratosphere is the layer above the troposphere that extends to 45–50 km altitude from the tropopause which separates troposphere and stratosphere. Ozone layer means that compared to troposphere below and mesosphere above a higher fraction of ozone molecules is found in the stratosphere between 15–30 km altitude. Since ozone in troposphere is very less and 90% of all atmospheric ozone is in stratosphere, this altitude region of stratosphere is called ozone layer. Ground level ozone or tropospheric ozone is a greenhouse gas, a pollutant, a health hazard and harmful to plants and materials and therefore, increase in ozone in troposphere is a cause of concern. On the other hand, stratospheric ozone is very much necessary for life on earth, because, here it filters out photons with shorter wavelengths (less than 320 nm) of ultraviolet (UV) rays (270–400 nm) from the sun that would be harmful to most forms of life in large doses. These same wavelengths are also among those responsible for the production of vitamin D in humans. In troposphere or lower atmosphere, when NO_x and VOCs react in the presence of sunlight, they form photochemical smog, a significant form of air pollution, especially in the summer. NO_x, CO and VOCs are called ozone precursors and it is known that motor vehicle exhaust, industrial emissions and chemical solvents are the major anthropogenic sources of these chemicals. When stagnant air masses linger over urban areas, the pollutants are held in the place for long time. Sunlight interacts with these pollutants that forms airborne particles called particulate matters and ground level ozone which is a major component of smog. It is established that at lower altitudes, ozone is produced via photochemical decomposition of NO_2 followed by three body reaction of atomic oxygen with O_2 as shown below:
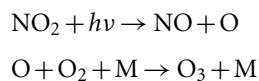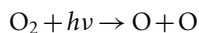
$$NO_2 + h\nu \rightarrow NO + O$$

$$O + O_2 + M \rightarrow O_3 + M$$

where M is any third body such as N_2 or O_2 that removes the energy of the reaction and stabilizes O_3.[37,40] The nitric oxide produced in this reaction reacts rapidly with ozone to regenerate NO_2 which is given below:

$$NO + O_3 \rightarrow NO_2 + O_2.$$
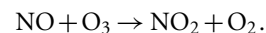
In final stage, NO_2 is regenerated and therefore, it is available to repeat the process. The above reactions occur rapidly establishing a steady state ozone concentration. The second and third reactions are comparatively fast and slower photolysis of NO_2 reaction is the rate determining step and that is why ozone is not formed appreciably at night. It is also one of the reasons why ozone concentration is high in the lower atmosphere during summer months, when temperature are high and solar radiation is intense. An increase in temperature also accelerates photochemical reaction rates. With higher temperatures, we can expect a larger number of 'bad ozone' days. Recent studies in southern California shows that amount of NO_x, CO, VOCs and PM are less at weekends compared to weekdays during ozone season from 1995 to 2001 and consequently, ozone concentration decreases at weekends.[41] In an investigation on ground level ozone concentration in Kathmandu valley in Nepal proves that the ozone concentration is strongly influenced by meteorological conditions such as temperature, solar radiation and prevailing levels of NO_x and also it varies in different days such as weekdays, weekends, clear days, cloudy days, general strike days, premonsoon and rainy season.[42] However, smoggy days, in general have bad effects on human health. People with lung diseases such as asthma and people who work or exercise outside are susceptible to adverse effects of smog such as damage to lung tissue and reduction in lung function. NO_2 could also be generated from the reaction of NO with peroxy radicals produced from the reaction of hydroxyl radical (OH) with hydrocarbons, CO and VOCs. From scientific view point, air pollutant ozone in troposphere should not be confused with the ozone layer in the stratosphere. In the stratosphere, ozone forms through the splitting of O_2 molecules by sunlight as it does in the troposphere near the earth's surface. However in the troposphere, nitrogen dioxide, not molecular oxygen, provides the primary source of the oxygen atoms required for ozone formation. Here, sunlight splits nitrogen dioxide into nitric oxide and an oxygen atom. In stratosphere, ozone is formed and consumed naturally by photochemical reactions involving UV radiation. Here, molecular oxygen interacts with UV radiation and splits into

oxygen atoms which either recombine to form O_2 or combine with O_2 in presence of a third body to form O_3 as written below:

$$O_2 + h\nu \rightarrow O + O$$

$$O + O_2 + M \rightarrow O_3 + M$$

where M is any third body such as N_2 or O_2 that removes the energy of the reaction and stabilizes O_3. Most of the ozone in the atmosphere is formed over the equator where amount of sunshine is highest throughout the year. Large scale air circulation patterns in the lower stratosphere move ozone towards the north and south poles, where its concentration builds up. Hence, highest amounts of ozone in the upper atmosphere (stratosphere) usually occur at high latitudes. Once formed, destruction of ozone in the stratosphere takes place as quickly as formation of ozone, because it is so reactive. Sunlight can readily split ozone into an oxygen molecule and an individual oxygen atom followed by the formation of two O_2 molecules as given below:

$$O_3 + h\nu \rightarrow O_2 + O$$

$$O + O_3 \rightarrow 2O_2.$$
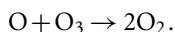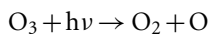
Thus, the ozone formation–destruction process in the stratosphere occurs rapidly and constantly, maintaining an ozone layer. The first of these two reactions serves to regenerate atomic oxygen for the second reaction which converts the ozone back to molecular oxygen. This second reaction is very slow. It can be enormously accelerated, however, by catalytic reactions. In the absence of such catalytic reactions, ozone could survive for 1–10 years in the stratosphere region. Later reaction could be catalyzed by trace gases such as nitric oxide (NO), nitrogen dioxide (NO_2) and nitrous oxide (N_2O) or simple molecules or free radicals of the halogens, including fluorine, chlorine and bromine. At any time, the formation and consumption of ozone proceed simultaneously. The actual concentration of ozone is a net function of the rates of reactions by which it is formed and the rates of the reactions that consume this gas. All the above molecules or free radicals catalyze the O_3 dissociation reaction rate leading to ozone layer depletion in stratosphere.[43] It has been discovered that man made chlorofluorocarbons (CFCs) producing chlorine free radical in presence of UV radiation are primarily responsible for the rapid catalytic destruction of ozone in the stratosphere.[37,44−46] CFCs also known as freons have been used in refrigeration, coolants and aerosols since 1930s and have a lifetime of about 20–100 years and could therefore continue to destroy ozone for a long period of time, so it pose a major problem. However, NO_x which is known as a significant auto exhaust pollutant also catalyzes ozone layer depletion in the stratospheric region through the reactions as given below:

$$NO + O_3 \rightarrow NO_2 + O_2$$

$$NO_2 + O \rightarrow NO + O_2.$$
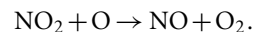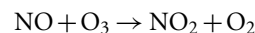
These reactions are largely responsible for ozone decline in middle to high altitudes from spring to fall. NO_x eventually form nitric acid when dissolved in atmospheric moisture forming a component of acid rain particularly in urban and industrial areas. The following chemical reaction occurs when nitrogen dioxide reacts with water:

$$2NO_2 + H_2O \rightarrow HNO_2 + HNO_3.$$
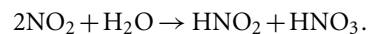
Nitrous acid then decomposes as follows:

$$3HNO_2 \rightarrow HNO_3 + 2NO + H_2O$$
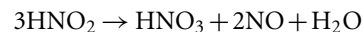
where nitric oxide will oxidize to form nitrogen dioxide that again reacts with water, ultimately forming nitric acid as follows:

$$4NO + 3O_2 + 2H_2O \rightarrow 4HNO_3.$$

NO_x react with ammonia, moisture and other compounds to form nitric acid vapor and related particles. Small particles can penetrate deeply into sensitive lung tissue and damage it, causing premature death in extreme cases. Inhalation of such particles for long time sometimes causes respiratory diseases such as emphysema, bronchitis and it may also aggravate existing heart disease. Peroxyacetyl nitrates (PAN) could also be generated from NO that contribute significantly to global photo oxidation pollution.[14] Biologically active NO is a poisonous product of in-vivo enzyme catalyzed transformation of amino acid, arginine. NO difuses through the alveolar cells and capillary vessels of the lungs and damages the alveolar structures and their functions throughout the lungs provoking both lung infections and respiratory allergies like bronchitis and pneumonia.

CO is a colorless, odorless gas and generally known for its extreme toxicity. It combines with hemoglobin to produce carboxyhemoglobin that is ineffective for delivering oxygen to tissues present in our body. Concentration as low as 667 ppm might cause upto 50% of the body's hemoglobin to convert to carboxyhemoglobin. In the US, National Institute

for Occupational Safety and Health (NIOSH) has established a recommended exposure limit (REL) for CO of 35 ppm as an 8 h time-weighted average (TWA) concentration. Situation could be dangerous beyond this exposure level.

Sulfur present in fuels gets oxidized to SO_2 and further oxidation of SO_2 followed by the reaction with H_2O eventually forms H_2SO_4 that also produces acid rain which is written as follows:

$$SO_2 + H_2O \rightarrow H_2SO_3$$
$$SO_2 + O_3 \rightarrow SO_3 + O_2$$
$$SO_3 + H_2O \rightarrow H_2SO_4.$$
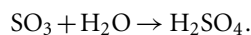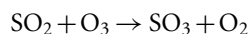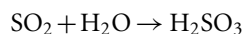
This acid generated from acid rain may be carried to the ground in rain or snow, but often particles containing sulfuric acid settle out of dry air. So the problem of the acid rain is really one of acid deposition in dry weather as well as wet. Acid rain has been held responsible for damaging buildings and statues made of limestone, damaging aquatic life in lakes, causing a decline of the plant growth in US and European forests and it might harm human health.

Particulates, alternatively known as particulate matters (PM) or fine particles, are tiny subdivisions of solid or liquid matter suspended in a gas or liquid. Size ranges of particulate matters are from less than 10 nm to more than 10 μm. PM_{10} is used to describe particles of 10 μm or less and $PM_{2.5}$ represents particles of 2.5 μm or less. Particles emitted from modern diesel engines that is commonly referred to as diesel particulate matters (DPM) or soot are typically in the size range of 100 nm. Larger particles are generally filtered in the nose and throat and do not cause problems, but particulate matters smaller than about 10 μm can settle in the bronchi and lungs leading to serious health problems. The smallest particles, less than 100 nm, may be even more damaging to the cardiovascular system. There is evidence that particles smaller than 100 nm can pass through cell membranes and migrate into other organs, including the brain. In addition, these soot particles also carry carcinogenic components like benzopyrenes adsorbed on their surface.

3. Global concern and legislations

In the early 1950's, air pollution and cars were first correlated by California researchers who established that huge traffics were to blame for the smoggy skies over Los Angeles area.[47–51] Since then, international concerns over the aspects of environmental pollution caused by polluting sources have been increasing and therefore, several global leaders mainly from developed countries have

been meeting at different timeframes to execute the regulations for controlling pollutants those are big threats for earth's air and ecology and health of living beings. Because pollutants can be carried many hundreds of kilometres by wind, thereby pollutants emitted in one country may be deposited in other countries.[52] Deposition of pollutants in a country can far exceed the amount of such pollution produced domestically due to pollution arriving from one or more upwind countries. In 1976, the Nordic environment ministers proposed a European convention on transboundary air pollution that emphasized sulphur compounds which is called Convention on Long-range Transboundary Air Pollution (CLRTAP). After negotiations, 34 countries and the European Commission signed the Geneva Convention in 1979. The convention came into force in 1983 and has now been ratified by 47 European countries along with US and Canada. In 1999, Gothenburg Protocol is signed in Gothenburg, Sweden to support CLRTAP setting emission limits for NO_x, SO_x, VOC and NH_3 to be met by 2010. In the similar way, Kyoto Protocol (1997) and Copenhagen Summit (2009) under United Nations Framework Convention on Climate Change (UNFCCC) have been effective to combat environment pollution as well as global warming. Implementations and status reports of these UNFCCC projects have been published time to time by Intergovernmental Panel on Climate Change (IPCC) that is a scientific body tasked with evaluating the risk of climate change caused by human activity. IPCC was established in 1988 by the World Meteorological Organization (WMO) and the United Nations Environment Programme (UNEP). IPCC got Nobel Prize for peace in 2007.

Keeping reduction of pollutant gases into account, several developed and later, developing countries have adopted legislation for the control of exhaust emissions to reduce air pollution. Each of these countries has set particular emission standards by law for different kinds of vehicles according to their own country's situation. Emission standards set specific limits to the amount of pollutants that could be released into the environment. It is a limit that sets threshold amounts above which different types of emission control technology must be necessary. Standards generally regulate the emissions of NO_x, SO_x, PM or soot, CO and HCs.

In US, emission standards are managed on a national level by Environmental Protection Agency (EPA), whereas state governments and local governmental bodies play a subsidiary role. California state has passed its own more stringent vehicle emission standards set by California Air Resources Board (CARB). Automotive market in

California is one of the largest in the world and particularly Los Angeles metropolitan areas have severe automobile-driven air pollution problems and CARB imposes strict regulations over emission requirements that major automakers must meet if they want to sell their cars into California market. Therefore, it is regarded as one of the strictest standards in the world and other states in US also choose to follow either federal standard or the stricter California standard. States following California standards include Maine, Vermont, Massachusetts, Rhode Island, Connecticut, New York, New Jersey, Pennsylvania, Maryland, Oregon, Washington, Arizona, Washington DC and New Mexico and these states are frequently referred to as CARB states. Regulations of CARB have also influenced European Union emission standards. In US, clean air legislation was first enacted in 1955, followed by Air Quality Act 1967 and Clean Air Act Amendments 1970, 1977 and 1990. Several categories of new engines as well as vehicles such as car and light trucks, heavy duty truck and bus engines, mobile non road diesel engines, railway locomotives, marine engines, small spark ignited (SSI) engines, large spark ignited (LSI) engines and stationary diesel engines are subject to emission standards in US. Two sets of emission standards (Tier I and Tier II) for light duty vehicles in US were defined in Clean Air Act Amendments 1990.[53] Tier I standard was adopted in 1991 and was effective from 1994 until 2003, whereas Tier II standards are being implemented from 2004 to 2009. There is a subranking ranging from BIN 1-10 within Tier II. BIN 1 is defined as cleanest emission standard and the vehicle having BIN 1 is called zero emission vehicle (ZEV), whereas BIN 10 is regarded as dirtiest emission standard. Automotive emission standards for low emission vehicle program in California are more stringent than national Tier regulations. The major emission categories for low emission vehicle program include transitional low emission vehicle (TLEV), low emission vehicle (LEV), ultra low emission vehicle (ULEV), super ultra low emission vehicle (SULEV) and ZEV. New categories for 2010 to 2016 are inherently low emission vehicle (ILEV), partial zero emission vehicle (PZEV), advanced technology partial zero emission vehicle (ATPZEV) and national low emission vehicle (NLEV). These standards specifically restrict emissions of CO, SO_x, PM, HCHO, non methane hydrocarbons (NMHC) and non methane organic gases (NMOG). ZEV is strictly restricted to electric vehicles and hydrogen cars. Tier II regulations also defined restrictions for the amount of sulfur allowed in gasoline and diesel fuel, since sulfur can interfere with operation of advanced exhaust treatment systems such as selective catalytic converters and particulate filters. Future emission regulations will be more stringent imposed by CARB moving towards a ZEV. Heavy duty vehicles must be regulated with Tier III and Tier IV within 2014.

European Union has its own policies for emission standards that all new vehicles must meet. Emission standards are applicable for all road vehicles, trains, barges and mobile non road engines such as tractors. No standards are set for seagoing ships or aeroplanes. European emission standards define the acceptable limits for exhaust emissions of new vehicles sold in European Union member states. Currently, emissions of NO_x, NMHC, PM, CO and total hydrocarbon (THC) are regulated for most vehicles. The toxic emission standards are defined as Euro 1, Euro 2, Euro 3, Euro 4 and Euro 5 fuels for light duty vehicles, whereas the corresponding series of standards for heavy duty vehicles are Euro I, Euro II, Euro III, Euro IV and Euro V. The European Union is to introduce Euro 4 on 1st January 2008, Euro 5 and Euro 6 standards are effective on 1st January 2010 and 1st January 2014. But these dates have been postponed for two years to give oil refineries the opportunities to modernize their plants. A typical European Union emission standards is given in Table 4.[54]

Australia started certification for new motor vehicle emissions with Euro categories in early 2000s. Euro III came into effect on 1st January 2006 and following Euro standards are being introduced with European introduction dates.

In 1992, Japan adopted Motor Vehicle NO_x Law to curb NO_x. The regulation was imposed for Tokyo, Saitama, Kanagawa, Osaka and Hyogo as these areas were affected with significant air pollution due to NO_x emitted from motor vehicles. This regulation was amended in 2001 to add PM into the regulation along with stricter NO_x removal requirements.

In China, emission standards are governed by State Environmental Protection Administration (SEPA).[55] China started to regulate its first emission controls on automobiles in 1990s that was similar to Euro I and it was modified in 2004 to Euro II standard. Similarly, more strict National Standard III, equivalent to Euro III was effective in 2007. Beijing introduced Euro IV in 2008, whereas the rest of the country would adopt this in 2010. Legislation was adopted for all new passenger cars with SI engines in Hong Kong to meet Euro IV standard in 2006. To meet increasingly strict emission standards, manufacturers are developing low pollution vehicles using alternative power, such as compressed natural gas vehicles (CNGV), liquefied petroleum gas vehicles (LPGV), hybrid electric vehicles (HEV), fuel cell vehicles (FCV) and electric vehicles (EV).

Table 4: European Union emission standards for gasoline and diesel powered (within bracket) passenger cars (g km^{-1}).

Tier	Timeframe	CO	THC	NMHC	NO$_x$	HC + NO$_x$	PM
Euro 1	July 1992	2.72 (2.72)	– (–)	– (–)	– (–)	0.97 (0.97)	– (0.14)
Euro 2	January 1996	2.2 (1.0)	– (–)	– (–)	– (–)	0.5 (0.7)	– (0.08)
Euro 3	January 2000	2.3 (0.64)	0.20 (–)	– (–)	0.15 (0.50)	– (0.56)	– (0.05)
Euro 4	January 2005	1.0 (0.50)	0.10 (–)	– (–)	0.08 (0.25)	– (0.30)	– (0.025)
Euro 5	September 2009	1.000 (0.500)	0.100 (–)	0.068 (–)	0.060 (0.180)	– (0.230)	0.005 (0.005)
Euro 6	September 2014	1.000 (0.500)	0.100 (–)	0.068 (–)	0.060 (0.080)	– (0.170)	0.005 (0.005)

In China, CNGVs and LPGVs are currently the most practical and popular clean vehicles. In the future, the government plans to develop EVs driven by storage batteries for buses and other public transportation vehicles, to encourage the production of HEVs for buses, to promote the innovation of FCVs as a longterm strategy, to strive for commercial use of FCVs by 2010 and to establish a methanol production and supply system to facilitate the introduction of FCVs.

India passed regulations for controlling emissions in 1991 and since 2000 it has started to adopt European emission standard for four wheeler light duty and heavy duty vehicles. Indian own emission standards will apply to two and three wheeled vehicles. National Auto Fuel Policy announced in 2003 envisaged a phased program for introducing Bharat Stage II to IV standards which are similar to Euro 2 to Euro 4 emission standards by 2010. These standards are applicable to all four wheelers sold and registered in the areas like National Capital Region (Delhi, Gurgaon, Faridabad, Noida and Ghaziabad), Mumbai, Kolkata, Chennai, Bangalore, Hyderabad, Ahmedabad, Pune, Surat, Kanpur and Agra. Bharat Stage III (Euro 3) standard for 2 and 3 wheelers would come into effect between 2008 and 2010. A typical Indian emission standards is summarized in Table 5.[56]

4. Technologies developed for controlling auto exhaust emission

4.1. *Processes for controlling pollution from auto exhaust*

As the concern about global and regional environmental problems continues to grow, enormous efforts have been made in last several years to advance the scientific and technological development for controlling auto exhaust emission. Some of invented technologies are briefly discussed below:

(a) Improvement in the engine design — Engine efficiency could be steadily improved with modified engine design, more precise ignition timing, electronic ignition and computerized engine management. Improvements in engine and vehicle technology continually reduce the toxicity of exhaust leaving the engine, but these alone have generally been proved insufficient to meet emission standards.

(b) Air injection — One of the first exhaust emission control systems is secondary air injection into each of the exhaust ports of an engine. The fresh air entering the hot exhaust manifold provides oxygen to burn any remaining fuel before it can exit the tailpipe. It was popular in the early 1990s before the extensive use of catalytic converters and now it is employed to reduce start up emissions.

(c) Fuel injection — The primary emission control is fuel injection. Fuel injection offers precise fuel control over a wide range of conditions. Feedback supplied by exhaust gas oxygen sensor and various engine sensors allows the injection system to compensate for changes in atmospheric conditions (temperature, altitude) as well as mechanical conditions (such as state of tune).

(d) Exhaust gas recirculation — Many engines produced after the 1973 model year have an exhaust gas recirculation (EGR) valve between the exhaust and intake manifolds. The valve opens under certain conditions to admit exhaust into the intake tract. Exhaust is largely inert, it neither burns nor supports combustion, so it dilutes the incoming A/F mixture to reduce peak combustion chamber temperatures. This, in turn, reduces the formation of NO$_x$. The EGR valve is the main control device in this system.

Table 5: Indian emission standards for four-wheeler vehicles.

Standard	Reference	Timeframe	Region
India 2000	Euro 1	2000	Nationwide
Bharat Stage II	Euro 2	2001	NCR*, Mumbai, Kolkata and Chennai
		April 2003	NCR, Mumbai, Kolkata, Chennai, Bangalore, Hyderabad, Ahmedabad, Pune, Surat, Kanpur and Agra
		April 2005	Nationwide
Bharat Stage III	Euro 3	April 2005	NCR*, Mumbai, Kolkata, Chennai, Bangalore, Hyderabad, Ahmedabad, Pune, Surat, Kanpur and Agra
		April 2010	Nationawide
Bharat Stage IV	Euro 4	April 2010	NCR*, Mumbai, Kolkata, Chennai, Bangalore, Hyderabad, Ahmedabad, Pune, Surat, Kanpur and Agra

*NCR stands for National Capital Region (Delhi, Gurgaon, Faridabad, Noida, and Ghaziabad).

(e) Catalytic converters — The catalytic converter is a device placed in the exhaust pipe that converts NO_x, CO and unburned HCs into benign gases by using different kind of catalysts.

(f) Evaporative emission control — Evaporative emissions are the result of raw fuel vapors escaping from the vehicle's fuel system. The emissions generated from the evaporation of raw fuel such as gasoline are controlled by the use of a closed ventilation system for the fuel tank or carburetor bowl vent on carbureted vehicles and a canister filled with activated charcoal to capture the fuel vapors. The charcoal canister captures and stores the vapors as they expand. When the engine is started, a purge control valve is opened allowing the engine to draw fresh air through the charcoal canister, pulling the vapor into engine, where it is burned. Since 1970, all US vehicles have had fully sealed fuel systems that do not vent directly to the atmosphere.

(g) Improvement in road condition and traffic network — Driving style can have an important influence on exhaust emission and fuel consumption. Good roads and changes in traffic network configurations improve overall flow of vehicles. This could lead to the reduction in emissions per vehicle kilometer traveled by decreasing the number of acceleration and deceleration events. Therefore, traffic signals or traffic jams due to congested roads should be replaced by roundabouts or flyovers. It is also observed that NO_x emission increases and CO, PM and HC emissions decreases with increase in engine temperature or increase in vehicle speed. Hence, there must be speed limit on the road, especially on the highway where numbers of vehicles are more. Some researchers argue that smooth flow of vehicles might generate extra traffic in that section causing more pollution and therefore, they claim that pollution impacts of traffic signals are highly situation specific.

4.2. *Catalytic converter*

Among all the types of technologies developed so far, use of catalytic converters is the best way to control auto exhaust emission. A catalytic converter (colloquially called catcon) is a device that usually reduces the toxicity of exhaust emissions generally from gasoline engines. A catalyst housed inside a catalytic converter performs chemical reactions by which pollutant combustion by-products are converted to less-pollutant substances. It was first widely introduced in automobiles in the US market in 1975 to comply with tightening EPA regulations on auto exhaust and catalytic converters are still most commonly used in motor vehicle exhaust systems for controlling emission. Catalytic converters are also used on trucks, buses, trains, mining equipments, generators and other engine-equipped machines. The catalytic converter was invented by Eugene Houdry, a French mechanical engineer who lived in the US. When the results of early studies of smog in Los Angeles were published in early 1950s,[47–51] Houdry became concerned about the role of automobile exhaust in air pollution and established a company, *Oxy-Catalyst*, to develop catalytic converters for gasoline engines and he obtained a patent (US2742437) for his invention of catalytic converter. But it was not that much useful until the extremely effective anti-knock agent tetra-ethyl lead was eliminated from most gasoline over environmental concerns that would poison the converter by forming a coating on the catalyst's surface, thereby effectively disabling it. The catalytic converter was later on further developed by John J. Mooney and Carl D. Keith at the Engelhard Corporation, starting the first production of catalytic converter in 1973.
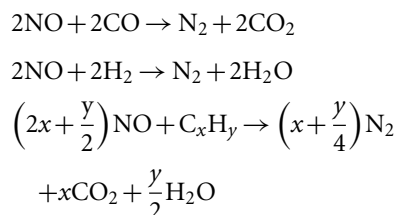
Since then catalytic converters have undergone several stages of development over the years. There have been two types of catalytic converters:

(a) Two-way catalytic converters are widely used on diesel engines to reduce hydrocarbon and carbon monoxide emissions. They were also used on spark ignited gasoline engines in US automobile market through 1981. But this two-way converter is unable to control NO_x and three-way catalytic converters come into the scenario. It has two simultaneous tasks such as (i) oxidation of CO to CO_2 and (ii) oxidation of unburned hydrocarbons to CO_2 and H_2O.
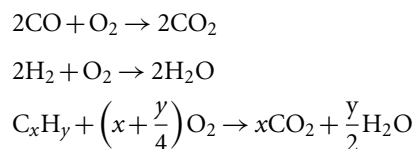
(b) Three-way catalytic converters have been used in vehicle emission control systems in North America and many other countries on roadgoing vehicles since 1981. A three-way catalytic converter has three simultaneous tasks, namely (i) oxidation of CO to CO_2 and (ii) oxidation of unburned hydrocarbons to CO_2 and H_2O and (iii) reduction of nitrogen oxides to nitrogen and oxygen.

The essential requirement for the catalyst employed in the present-days catalytic converter for gasoline engine is to cater the high conversion of NO_x, CO and HCs present in the auto exhaust gases to inert and harmless N_2, CO_2 and H_2O. The overall catalytic reactions which are important for controlling auto exhaust emissions are given by the following stoichiometric equations:
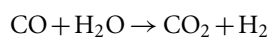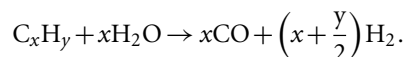
a) reduction reactions

$$2NO + 2CO \rightarrow N_2 + 2CO_2$$

$$2NO + 2H_2 \rightarrow N_2 + 2H_2O$$

$$\left(2x + \frac{y}{2}\right)NO + C_xH_y \rightarrow \left(x + \frac{y}{4}\right)N_2$$

$$+ xCO_2 + \frac{y}{2}H_2O$$

b) oxidation reactions

$$2CO + O_2 \rightarrow 2CO_2$$

$$2H_2 + O_2 \rightarrow 2H_2O$$

$$C_xH_y + \left(x + \frac{y}{4}\right)O_2 \rightarrow xCO_2 + \frac{y}{2}H_2O$$

c) water gas shift reaction (WGSR)

$$CO + H_2O \rightarrow CO_2 + H_2$$

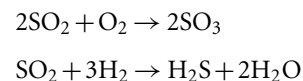d) steam reforming reaction

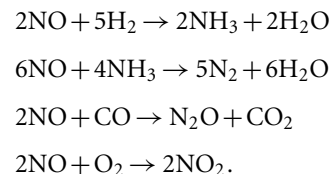$$C_xH_y + xH_2O \rightarrow xCO + \left(x + \frac{y}{2}\right)H_2.$$

However, depending on the operating conditions of the catalyst a number of secondary reactions might occur. The most common of these are:

a) reactions with SO_2

$$2SO_2 + O_2 \rightarrow 2SO_3$$

$$SO_2 + 3H_2 \rightarrow H_2S + 2H_2O$$

b) reactions with NO

$$2NO + 5H_2 \rightarrow 2NH_3 + 2H_2O$$

$$6NO + 4NH_3 \rightarrow 5N_2 + 6H_2O$$

$$2NO + CO \rightarrow N_2O + CO_2$$

$$2NO + O_2 \rightarrow 2NO_2.$$

Moreover, removal of NO from auto exhaust emission could also be achieved by selective catalytic reduction (SCR) of NO to N_2 using NH_3. Other reductants such as H_2, CO and hydrocarbons are also used for SCR of NO. The main reactions involved in SCR are:

$$4NO + 4NH_3 + O_2 \rightarrow 4N_2 + 6H_2O$$

$$6NO_2 + 8NH_3 \rightarrow 7N_2 + 12H_2O.$$
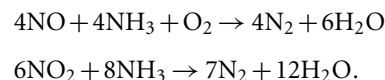
All the above reactions required some heat or temperature on the catalyst surface for the reaction to occur. When automobile first starts, both the engine and catalyst are cold. After start up, heat of combustion is transferred from the engine and the exhaust piping begins to heat up. Finally, a temperature is reached within the catalyst that initiates the catalytic reactions. This light-off temperature depends on the chemistry of the catalyst. Typically CO reaction begins first followed by HC and NO_x reactions.

The sale of diesel vehicles is increasing dramatically due to its cost effectiveness and decrease in emission of green house gases, especially CO_2. In traditional stoichiometric gasoline engines the combustion mixture always contains sufficient oxygen to combine with the fuel. On the other hand, in a diesel engine, oxygen is always in excess, since only sufficient diesel fuel is injected into a highly compressed hot air in the cylinder to produce the power at a particular instant. Thus, unlike gasoline engine, diesel engine is a compression-ignition process. Its lean nature results in a cooler combustion with less NO_x formation. Here role of catalyst is to reduce soluble organic fraction (SOF) and gaseous CO and HC emission, but specifically selective to minimize the oxidation of SO_2 to SO_3 leading to H_2SO_4. Thus, the challenges for catalysts are quite demanding and different from that for its gasoline counterpart, because catalysts with high activity for oxidizing SOF would likely be good catalysts for SO_2 to SO_3. For diesel engines,

the most commonly used catalyst in the catalytic converter is the diesel oxidation catalyst. This uses excess O_2 in the exhaust gas stream to oxidize SOF to CO_2 and H_2O, CO to CO_2 and hydrocarbons to H_2O and CO_2. In the early 1990s the diesel engine manufacturers, being aware of the successes of the catalytic converter for the gasoline engine, considered a catalyzed flow-through monolith for controlling emissions from their engines. Diesel engines run in lean conditions and therefore are much cooler than modern stoichiometrically operated gasoline engines and thus, even if SOF from diesel engine are gaseous or aerosols they are quickly cooled and condensed in this idle or low power output conditions. The catalyst would therefore have to function at much lower temperatures than in the gasoline counterpart and would be required to treat liquids as well as gases. The catalyst also must have high selectivity towards the oxidation of gaseous CO and HC while not oxidizing SO_2. These converters often reach 90% efficiency, virtually eliminating diesel odor and helping to reduce visible particulates (soot). However they are incapable of reducing NO_x in lean-burn condition as chemical reactions always occur in the simplest possible way and the existing O_2 in the exhaust gas stream would react first. To reduce NO_x on a diesel engine, the chemical composition of the exhaust must first be changed. Two main techniques such as SCR of NO and NO_x traps or NO_x absorbers are used. Diesel engine exhaust contains relatively high levels of particulate matter (PM) or soot, consisting in large part of elemental carbon. Catalytic converters cannot clean up elemental carbon, so particulates are cleaned up by a soot trap or diesel particulate filter (DPF). In US, all on road heavy duty vehicles powered by diesel and built after 1st January 2007 must be equipped with a catalytic converter and a DPF. The most satisfactory way of removing trapped PM is to oxidize it to CO_2 and H_2O. The PM can be almost completely removed from the exhaust stream using a DPF. This trapped PM can then be combusted using either NO_2 (at low temperatures, 250–300 °C and above), or O_2 (at high temperatures, 550–600 °C). On heavy duty diesel vehicles, such as trucks and buses, the engine is often working at high load and the exhaust temperature is in the range 250–400 °C. Under these conditions it is possible to use the already present NO in the exhaust gas in a process that continually oxidizes trapped PM. An oxidation catalyst upstream of the filter oxidizes HCs and CO to CO_2 and H_2O and also converts NO to NO_2 that is very powerful oxidant and continually removes PM. Details of modern-days catalytic converters and its scientific and technological aspects have been reviewed in several articles.[22,30–32,57–61]

4.3. Controlling pollution from cold-start emission

It has been established that 60–80% of unburned HCs and CO are emitted from a motor vehicle equipped with a three way catalyst (TWC) within first few minutes or approximately first few kilometers after vehicle starts.[62–64] This period is called cold-start condition and the emission occurred during this period is called cold-start emission. Under cold-start conditions, the engine has to overcome larger frictional forces in its moving parts that requires to introduce a substantially larger amount of fuel than the stoichiometric proportion in order to guarantee prompt vaporization and starting and the TWC is totally inactive, because the catalytic converter has not yet warmed up. Together, these two important factors are responsible for the higher tailpipe emission during cold-start phase. The extent of this cold-start phase is also dependent on the outside temperature and characteristics of the vehicle. TWCs in catalytic converters used in motor vehicles presently are able to achieve the reductions of CO, NO_x and unburned HCs by up to 95% when they are full warmed up. TWC will not be able to function effectively until it reaches the light-off (operating) temperature as the conversion efficiency depends strongly on the working temperature and is practically zero during the starting and warming up period. The process of catalyst warm up is typically referred to as light-off. Some researchers refer to the catalyst warm up time from almost zero efficiency at cold-start to 50% conversion efficiency as the light-off time. Typically it is necessary to reach 350 °C for light-off to occur. The delay until it reaches operating temperature leads to high levels of tailpipe emissions especially hydrocarbons. Many distances driven are so short that the end of the cold-start phase is either not reached or just about reached. Short journeys, mostly consisting of home to work place, home to various service units in the city such as post office and bank, home to school, home to local shops, home to doctor's chamber have large average fuel consumption and emission values (g km^{-1}) due, essentially to cold-start. Average trip length in Europe is only about 5 km and about 50% of city driving is 2 km or even less. On average the cold distance defined as the distance necessary for cold tailpipe emissions to reach hot emission levels is typically within 5 km. That indicates that a large amount of urban driving occur in cold condition. This scenario is even worse at low ambient temperature.[65] Cold-start emission of pollutant gases from vehicles is thus one of the most severe problems in large cities, where the number of vehicles and daily engine startings per populated area is high. Hence, minimizing

emission of pollutants mainly, HCs in the cold-start period is very critical for getting very low tailpipe emission. Therefore, in recent years, there are efforts to reduce tailpipe emission during cold-start in order to achieve low emission vehicles. As a result, both US and European emission standards include cold-start operation tests using US 1975 Federal Test Procedure (FTP 75), Economic Commission for Europe (ECE) and New European Driving Cycle (NEDC) at ambient temperatures of 20–30 °C (68–86 °F), before the catalytic converter is warmed up. Especially, the Euro III and Euro IV emission standards have included a subambient cold-start test at a temperature of −7 °C, during the first 780 s of the urban driving cycle, limiting HC and CO tailpipe emissions in such conditions.

The technology to develop suitable methods to control cold-start emission having both catalytic as well as some unique techniques includes (a) close-coupled catalyst, (b) electrically heated catalyst, (c) hydrocarbon trap, (d) chemically heated catalyst, (e) employing partial oxidation catalyst, (f) exhaust gas ignition, (g) pre-heat burners, (h) cold-start spark retard or post manifold combustion, (i) variable valve combustion chamber (j) double walled exhaust pipe and (k) electronic ignition system.[66–72] All these approaches contain underfloor catalysts of various compositions.[73] It has been established that development of high temperature close-coupled catalyst is the leading technology for most LEV, ULEV and SULEV applications. Close-coupled catalyst near the engine manifold has been used for removal of HCs, whereas the underfloor catalyst removes remaining CO and NO_x. Another prominent approach is the use of hydrocarbon trap in which the cold HCs are adsorbed and retained on an adsorbent until the catalyst reaches the light-off temperature. Cold-start phase could also be overcome by using electrically heated catalyst (EHC). During start up period exhaust gas or catalyst surface could be heated by resistive materials and a current/voltage source that could reduce the time required for catalyst light-off. EHC is placed in front of light-off catalyst that receives the pre-heated gas and thus, provides very efficient reaction in the cold-start period.

5. Catalysts for controlling auto exhaust pollutants

5.1. *Present conventional catalysts for the abatement of auto exhaust emission*

Generally, metal, alloy and metal oxide catalysts were used for exhaust emission catalytic reactions in early days. Basic studies on metal catalysts involve single crystal or polycrystalline forms of bulk metal such as powder, wire, foil or ribbons. Prominent

metals used are Pt, Pd, Rh, Ru and Ir. CuO, Fe_2O_3, TiO_2, V_2O_5, MoO_3, WO_3, Cr_2O_3 and Al_2O_3 are employed as oxide catalysts.[74]

Transition metal ion exchanged zeolites have also been developed for SCR of NO. Copper is one of the promising elements which has the ability to increase the SCR activity of NO with NH_3. Cu^{2+} ion exchanged Y zeolite, mordenite, ZSM-5 and MFI-ferrisilicate have been found to be effective SCR catalysts for NO. Other metal ions such as Fe^{3+}, Co^{2+}, Ce^{4+} and Ag^+ exchanged zeolites also show good SCR activity for NO. Noble metal exchanged zeolites are active for the removal of NO.[74]

The catalytic reduction of NO, oxidation of CO and hydrocarbons have also been carried out over pure and cation substituted perovskite such as $LaCoO_3$, $LaMnO_3$, $Ln_{1-x}Pb_xMnO_3$ (Ln = La, Pr and Nd), $LaMn_{1-x}Cu_xO_3$ and $La_{1-x}Sr_xMnO_3$. They have different cationic sites in the crystal structure which are highly amenable to substitution. Usually metals of high oxidation states can be stabilized in perovskite structure. A large number of spinels, AB_2O_4 (A = Mg^{2+}, Co^{2+}, Ni^{2+}, Cu^{2+} and Zn^{2+} and B = Al^{3+}, Cr^{3+}, Mn^{3+}, Fe^{3+} and Co^{3+}) are also employed for NO reduction and CO and hydrocarbon oxidation.[74]

In early 1980s, supported metal catalysts have come in the scenario of auto exhaust catalysis.[75–79] Metal catalysts with low metal loading are usually dispersed on the surface of a support. Highly dispersed catalysts provide a maximum surface area. As metal loading increases the crystallites come closer together causing larger particle size. Generally, the more expensive precious metal catalysts have low metal loading and are highly dispersed, whereas catalysts containing less expensive base metals have higher metal loadings, usually 20–40% by weight or atom. In particular, present-days automotive exhaust catalysts revolves around three noble metals such as Pt, Pd and Rh that have been dispersed, stabilized, promoted, alloyed and segregated in sophisticated ways over the years to fulfill the required performance and γ-Al_2O_3 has been found to be the main support.[24] Current auto exhaust catalyst consists of noble metal particles, mainly Pd to the extent of 2% by weight along with Pt and Rh possible to the limit of 0.5% each dispersed over high surface area γ-Al_2O_3 mixed with 30% by weight of $Ce_{0.7}Zr_{0.3}O_2$ as oxygen storage material.[24]

### 5.2. *Importance of oxygen storage in auto exhaust catalysis and role of CeO_2*

Since early 1980s catalytic converter with three way catalyst (TWC) has been regarded as a major breakthrough in the development of device for the controlling of auto exhaust emission. TWCs

are capable of converting CO, HC and NO_x into benign CO_2, H_2O and N_2 simultaneously and efficiently, provided that A/F ratio is constantly kept in the exhaust at the stoichiometric point (14.7) where concentrations of oxidizing and reducing gases are equal. High efficiency of conversion is achieved over TWC in a very narrow A/F window that requires a highly efficient control of exhaust composition, particularly in terms of residual oxygen concentration. Strong deviations or oscillations of A/F from the stoichiometric value lead to widening of operating window resulting in an average poor performance of TWC. The engines with earliest catalytic emission control systems were fuelled through carburetor or fuel injection device, but precise control of the amount of fuel that mixed with intake air could not be done by this system. Therefore, for widespread application of TWC, controlling of A/F ratio has been required further development on the basis of engineering as well as chemical control. Present integrated TWC system contains (a) an oxygen sensor in the exhaust to provide an electrical signal indicating the engine is running rich or lean, (b) electronic fuel injection (EFI) that could meter precise amounts of fuel providing a stoichiometric A/F mixture and (c) a microprocessor to control a feedback-loop using oxygen sensor signals to determine the amount of fuel injected under specific engine operating conditions to maintain stoichiometric conditions. In recent years, starting in California, vehicles are also required to have on-board diagnostic (OBD) systems for monitoring the performance of a number of emission related vehicle components and systems that contain different sensors for exhaust gas constituents (CO, HCs and NO_x).[80] However, the exhaust gases fluctuate between slightly rich to slightly lean conditions, with an inevitable time lag in the system as it adjusts the ratio electronically. This can decrease the conversion rate, especially when the difference between the degree of enrichment is large and the alternating period becomes long and hence, the range of A/F ratios should be widened to take dynamic driving into account. In this context, chemical control of A/F ratio comes into the picture. To widen the operating window for the catalyst, the exhaust gas composition on the catalyst must be controlled by storing oxygen in the oxygen-rich condition and by releasing oxygen in the oxygen-lean condition. This could be achieved by adding oxygen storage material in TWC which shows high oxygen storage capacity (OSC). This oxygen storage material readily undergoes reduction–oxidation cycles that provide oxygen for CO and HC oxidation in rich region and the reduced state can remove oxygen from gas phase

when the exhaust gas runs into lean region. Thus, an oxygen storage material not only widens A/F ratio window, but also promotes oxidation activity.

OSC is the ability to attenuate the negative effects of rich and lean fluctuation of exhaust gas composition upon pollutant conversion. It is a crucial property of TWC directly linked to its efficiency operating under fluctuating conditions. Generally, OSC is classified as total OSC and dynamic OSC.[81–83] Total OSC refers to the amount of oxygen thermodynamically available that has been investigated employing temperature programmed reduction (TPR), temperature programmed oxidation (TPO) and thermogravimetric (TG) studies.[84–87] TPR by H_2 or CO and oxidation by O_2 gives an estimate of OSC of an oxide. In this experiment, the rate of oxygen released from the oxide is measured as a function of temperature, under flowing hydrogen or carbon monoxide. The released oxygen can be estimated by the rate of consumption of hydrogen or carbon monoxide detected from the mass-spectral peak of water or carbon dioxide or by oxygen pump or by thermal conductivity detector (TCD).[88–90] On the other hand, dynamic OSC accounts for the amount of oxygen kinetically available during fast transitions between reduction and oxidation environments and it has been investigated using oxygen isotopic exchange, CO pulse and CO/O_2 pulse alternating at a given frequency measurement. Dynamic OSC provides better simulations of fluctuations that exhaust gas might undergo during real operation and is therefore, considerably more useful in the evaluation oxygen storage activity of the material.

Materials for TWC applications must fit very demanding kinetic and thermodynamic requirements. They should have redox behavior capable to release/uptake rapidly as much oxygen as possible leading to have high OSC. Utilization of lattice oxygen from reducible oxides under reducing condition and thereafter replenishment of oxygen under oxidizing atmosphere has played a critical role in various oxidation reactions.[91] Therefore, a reducible oxide with redox characteristics could act as both oxidizing and reducing agent to various reactants depending on the reaction condition. In this context, CeO_2 has been found as an efficiently suitable oxygen storage material for the wide application in TWC according to the following reversible reactions:

$$CeO_2 \rightarrow CeO_{2-\delta} + \delta/2O_2$$
$$CeO_{2-\delta} + \delta/2O_2 \rightarrow CeO_2$$
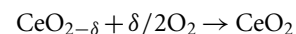
where first reaction is related to oxygen-lean region and second one is for oxygen-rich region and value

for δ is in between 0 and 0.25. Experimentally achieved δ is ~0.05 in the temperature range upto 600 °C.
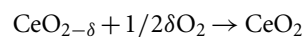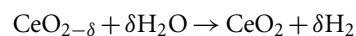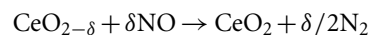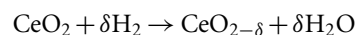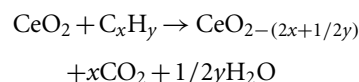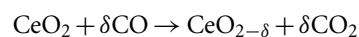
CeO_2 is usually treated as an active support for precious metal as well as base metal catalysts in heterogeneous catalysis.[92–94] It has been widely used as a promoter for TWC such as Al_2O_3 employed for the control of toxic emission from automobile exhausts for many years.[95, 96] It is observed that addition of ceria increases the activity of Al_2O_3 catalyst towards TWC. The promoting effect of CeO_2 is largely attributed to the enhancement of metal dispersions, OSC, increase in oxygen mobility due to oxide ion defects and thermal stability.[81,82,97] The ability of ceria to store/release oxygen is primarily caused by the fluorite crystal structure that it adopts and the presence of mixed valence of cerium, Ce^{4+} and Ce^{3+} leading to redox properties. The fluorite lattice having a metal ion of variable valency is flexible to release oxygen to accommodate significant amount of oxygen vacancies under reducing conditions. These vacancies will be refilled with oxygen atoms under oxidizing conditions. Hence, Ce^{4+} is reduced to Ce^{3+} in reducing atmosphere in CeO_2 and it is reoxidized to Ce^{4+} in oxidizing atmosphere. Therefore, CeO_2 is able to act as an efficient oxygen buffer by releasing/storing oxygen because of its capability to undergo effective reduction and reoxidation under fuel-rich (A/F < 14.7) and fuel-lean (A/F > 14.7) conditions. This reversible oxygen storage/release feature coupled with chemical stability in adverse conditions is a unique feature that offers ceria the prime position in TWC design. Generally, higher conversion efficiencies are obtained with higher OSC of the promoter. The process of oxygen storage and transport in CeO_2 occurs through the lattice oxygen defects. These defects could be either intrinsic or extrinsic depending on the mode of creation of oxygen vacancies. These oxygen defects play an important role in promoting the catalytic activity of CeO_2-based materials. In recent studies, it has been shown that incorporation of Zr, Y, La, Tb, Gd, Pb and Pr in CeO_2 leads to create oxygen vacancies improving the catalytic activity and redox properties to a considerable extent.[74] The enhancement in the activity is attributed to high oxygen ion mobility in the fluorite lattice. It has also been shown that activity of CeO_2 in redox reactions is enhanced not only by noble metals but also by base metal like copper. Martínez-Arias et al. and Flytzani-Stephanopoulos et al. have extensively investigated the promoting effect of CeO_2 in CuO/CeO_2, $Cu/CeO_2/Al_2O_3$, CeO_2/Al_2O_3 and Cu/CeO_2 regarding their catalytic behavior and redox properties.[98,99] The promoting effect in these catalysts has been correlated with the synergism of the redox properties of the system which is achieved by metal–ceria interaction.

The discovery of CeO_2 as oxygen storage material and support for heterogeneous catalysts led to enormous investigation since the early 1980s. However, OSC of CeO_2 for oxidation/reduction reaction was first time estimated in a H_2-TPR experiment on CeO_2 by Yao and Yao.[81] Simple mechanism of OSC from H_2-TPR could be written as:

$$CeO_2 + \delta H_2 \rightarrow CeO_{2-\delta} + \delta H_2O$$

$$CeO_{2-\delta} + \delta/2 O_2 \rightarrow CeO_2.$$
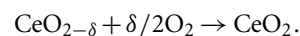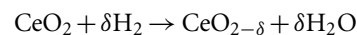
Unique redox property of ceria has made it a special component of three-ways catalysts, since it can store oxygen during lean (net oxidizing, excess of O_2) conditions and release it during rich (net reducing, deficient of O_2) conditions as given below:

$$CeO_2 + \delta CO \rightarrow CeO_{2-\delta} + \delta CO_2$$

$$CeO_2 + C_xH_y \rightarrow CeO_{2-(2x+1/2y)}$$
$$+ xCO_2 + 1/2y H_2O$$

$$CeO_2 + \delta H_2 \rightarrow CeO_{2-\delta} + \delta H_2O$$

$$CeO_{2-\delta} + \delta NO \rightarrow CeO_2 + \delta/2 N_2$$

$$CeO_{2-\delta} + \delta H_2O \rightarrow CeO_2 + \delta H_2$$

$$CeO_{2-\delta} + 1/2\delta O_2 \rightarrow CeO_2$$

H_2-TPR of CeO_2 shows primarily two peaks at approximately 500 and 825 °C.[81] The low temperature peak is due to the reduction of most easily reducible surface oxygen of CeO_2 while removal of bulk oxygen is suggested as the cause of high temperature at 825 °C. The first peak is dependent on the surface area and responsible for higher catalytic activity at lower temperature. There is a good correlation between BET surface area of CeO_2 and H_2 consumption. Higher surface area material means more surface oxygen can be removed by H_2 or CO gas in that material leading to higher OSC. In another kind of investigations, substitution of isovalent cations like Ti^{4+}, Zr^{4+}, Hf^{4+} and Th^{4+} ions forming $Ce_{1-x}M_xO_2$ solid solutions might be much more important in enhancing OSC. Substitution of Zr ion in CeO_2 showed much higher OSC as well as redox behavior.[82,83,100−102] It may be noted that ZrO_2 is not reducible by H_2 or CO but Zr substitution in Ce site in $Ce_{1-x}Zr_xO_2$ showed enhanced reduction of Ce^{4+} thus increasing OSC. In general, high surface area, oxygen vacancy and movement of oxide ions from tetrahedral sites

to vacant octahedral sites are the possibilities for enhancing the OSC. In another sense, $Ce_{1-x}Zr_xO_2$ and such oxygen storage materials are not the catalysts themselves for real applications. Noble metals such as Pt, Pd Rh, bimetallic Pt–Rh are dispersed mostly in the form of nanocrystalline metal particles on such OSC materials and they are used as catalysts. Often, $Ce_{0.7}Zr_{0.3}O_2$ is dispersed over γ-Al_2O_3 and noble metals are dispersed over this for catalytic use. Thus, real catalyst is quite complex and understanding their catalytic activity would involve structural study of such complex materials. Realizing the immense potential of substituted CeO_2 based materials regarding OSC as well as catalytic activity we have synthesized a series of doped CeO_2 compounds by solution combustion method and examined their OSC and several catalytic reactions related to auto exhaust catalysis which would be discussed in the following sections.[103,104]

5.3. New approach for developing novel catalysts

From basic view point of TWC it is necessary to develop such kind of materials that would provide unique OSC and active sites for redox type of exhaust catalytic reactions as both the properties are correlated. Over the years, it is established that metals are in general active sites for adsorption and catalysis and hence, most exhaust catalysts contain nanocrystalline noble metals (Pt, Pd and Rh) dispersed on supports like Al_2O_3 or SiO_2 promoted by CeO_2.[24] However, in conventional catalysts, noble metal atoms on the surfaces of the nano metal particles in their zero valent state serve as active sites for both oxidizing and reducing molecules. Even in 4–6 nm metal particles, only 1/4 or 1/5 of the total noble metals are utilized for catalytic conversion. If 6 nm Pt particle is considered, then number of Pt atoms would be $\sim$14800, where number of surface Pt atom would be only $\sim$2870. This means 1/5 of Pt atoms are available for adsorption. If all Pt atoms are utilized, then reaction rate would be higher by 5 times. Thus, catalytic activity increases with increase in metal dispersion. Atomic dispersion of noble metals on traditional supports like Al_2O_3 is difficult because metal atoms sinter into metal particles due to metal-metal bonding. The complete dispersion of noble metals could be achieved only as ions within a reducible oxide support.

Understanding the importance of CeO_2 as oxygen storage material as well as active catalysts for redox type exhaust catalytic reactions, an entirely new approach of synthesizing uniform solid catalysts comprising noble metal ions and CeO_2 support could be developed. Noble metal oxides such as PtO, PtO_2, PdO and Rh_2O_3 are known and therefore,

it should be possible to synthesize solid solution between CeO_2 and noble metal oxides. Noble metal loading in exhaust catalysts is only to the extent of 1–2 wt.% and hence substitution of only 1–2% noble metal ion in CeO_2 would be sufficient to develop a catalyst. The underlying principle of doping aliovalent metal ions into CeO_2 is to retain its parent structure. Thus, synthesis of single phase oxide, $Ce_{1-x}M_xO_{2-\delta}$ (M = noble metals) is a new concept which is the basis of metal ion catalysts. Similarly, substitution of noble metals in TiO_2 forming $Ti_{1-x}M_xO_{2-\delta}$ (M = noble metals) retaining anatase structure of TiO_2 is basic idea behind the noble metal ion dispersion in a reducible support oxide. It has been more than 10 years we have been following this novel approach to synthesize noble metal ionic catalysts by solution combustion method. Promoting action of CeO_2 and TiO_2, metal–support interaction, high OSC, hydrogen spillover and synergistic interaction could all be attributed to the interaction of M^0/M^{n+}, Ce^{4+}/Ce^{3+} and Ti^{4+}/Ti^{3+} redox couples in the noble metal ion substituted in a reducible oxides.

Substitution of noble metal ions in CeO_2 has been achieved for the first time by a novel solution combustion method.[105] The solution combustion method involves rapid heating at a particular temperature of an aqueous redox mixture containing stoichiometric amounts of corresponding metal salts and hydrazine based fuels and the product is formed within 5 min.[106] Redox compounds or mixtures containing hydrazide groups have been found useful for the combustion synthesis of oxide materials. An ideal fuel should be water soluble and have low ignition temperature ($<$500 °C). It should be compatible with transition metal nitrate so that the combustion can be controlled, smooth and does not lead to explosion. The merits of solution combustion technique are: (a) being a solution process, it has all the advantages of wet chemical process such as control of stoichiometry, doping of desired amount of impurity ions and forming nano size particles (b) low temperature initiated process, (c) highly exothermic due to redox reaction, (d) self propagating, (e) transient high temperature, (f) production of huge amount of gases, (g) simple, fast and economical and (h) formation of high surface area, voluminous and homogeneous product. The synthesis of fine noble metal ion CeO_2 solid solution by solution combustion synthesis is an accidental discovery. When an aqueous solution containing stoichiometric amounts of $Al(NO_3)_3$, H_2PtCl_6 and urea was heated rapidly, the solution boils, froths and burns with flame temperature of 1500 °C yielding nano sized Pt metal particles

Figure 1: Sequences of solution combustion synthesis.
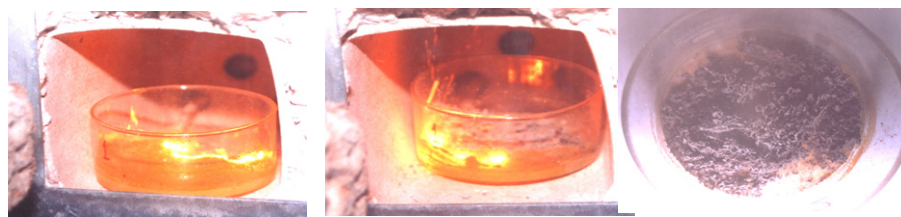
Figure 2: XRD of $Ce_{0.98}Pd_{0.02}O_{2-\delta}$.
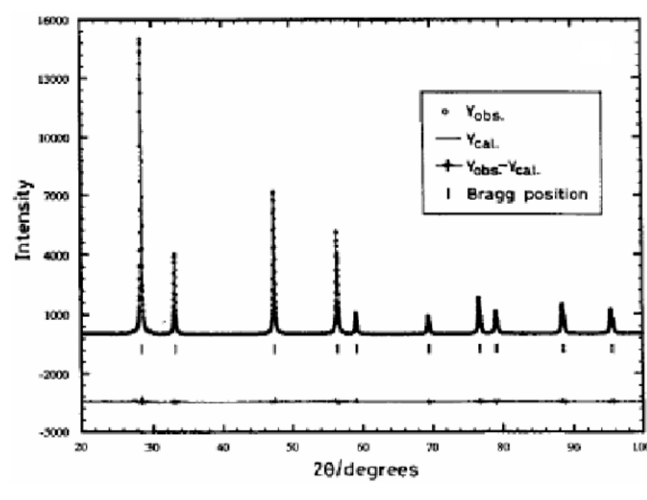
dispersed on α-Al_2O_3. On the other hand, Pt metal particles were not obtained when the same attempt was made to disperse 1–2% Pt metal in CeO_2 by the combustion of ceric ammonium nitrate, H_2PtCl_6 and oxalyldihydrazide ($C_2H_6N_4O_2$, ODH). Rather, 25–30 nm $Ce_{1-x}Pt_xO_{2-\delta}$ crystallites were formed where Pt ions are in +2 and +4 oxidation states. Figure 1 shows a typical sequence of the formation of a catalyst by solution combustion process. Combustion of $TiO(NO_3)_2$, noble metal salts and ODH fuel was employed for the preparation of $Ti_{1-x}M_xO_{2-\delta}$ catalysts and metal ion doped 5–10 nm TiO_2 in anatase phase was obtained. Table 6 summarizes metal ion substituted oxide materials prepared by solution combustion method.

5.4. Structure of $Ce_{1-x}M_xO_{2-\delta}$ and $Ti_{1-x}M_xO_{2-\delta}$ catalysts

Crystal structure, morphology, electronic structure, local structure and oxide ion vacancies of the catalysts have been evaluated by X-ray diffraction (XRD), transmission electron microscopy (TEM), X-ray photoelectron spectroscopy (XPS) and X-ray absorption fine structure spectroscopy (XAFS).

High resolution XRD data (Rigaku-2000) with rotating anode shows that CeO_2 crystallizes in fluorite structure where Ce^{4+} ions are cubic close packed with all tetrahedral sites occupied by oxygen. In 1 and 2% Pd/CeO_2, diffraction lines are indexed for fluorite structure and lines corresponding to Pd or PdO are not observed in the XRD patterns. Even a slow scan in Pd(111) region ($2\theta \approx 40 \pm 5°$) does not show any indication of Pd metal peak. In contrast, Pd/CeO_2 prepared by impregnation method shows diffraction lines due to Pd metal. Rietveld refinement shows that R factors are less than 1%. Lattice parameter decreases from 5.4113(2) Å in pure CeO_2 to 5.4107(3) Å in 2% Pd/CeO_2 confirming the substitution of Pd^{2+} ions (0.84 Å) for Ce^{4+} ions (0.99 Å) in CeO_2. Typical XRD pattern of 2% Pd/CeO_2 is shown in Figure 2. In 1% Pt/CeO_2, no impurity lines could be observed related to any platinum oxides, whereas a small broad hump at $2\theta = 39°$ due to Pt(111) could be seen in the diffraction pattern indicating the presence of trace amount of Pt. Comparing the intensity ratio of Pt(111) in 1% Pt/CeO_2 with that in 1% Pt + CeO_2 physical mixture it has been inferred

Table 6: Various metal ions substituted CeO_2 and TiO_2 based catalysts prepared by solution combustion method.

Metal ions	Support oxides				
	CeO_2	TiO_2	$Ce_{1-x}Ti_xO_{2-\delta}$	$Ce_{1-x}Zr_xO_{2-\delta}$	$Ce_{1-x}Sn_xO_{2-\delta}$
Cu^{2+}	$Ce_{1-x}Cu_xO_{2-\delta}$ ($x=0.01-0.1$)	$Ti_{1-x}Cu_xO_{2-\delta}$ ($x=0.2$)	$Ce_{0.8-x}Ti_{0.2}Cu_xO_{2-\delta}$ ($x=0.05, 0.1$)	$Ce_{1-x-y}Zr_xCu_yO_{2-\delta}$ ($x=0.25, y=0.02$)	
Ag^+	$Ce_{1-x}Ag_xO_{2-\delta}$ ($x=0.01$)	$Ti_{1-x}Ag_xO_{2-\delta}$ ($x=0.01$)			
Au^{3+}	$Ce_{1-x}Au_xO_{2-\delta}$ ($x=0.01$)				
Pd^{2+}	$Ce_{1-x}Pd_xO_{2-\delta}$ ($x=0.01, 0.02$)	$Ti_{1-x}Pd_xO_{2-\delta}$ ($x=0.01, 0.02$)	$Ce_{0.75-x}Ti_{0.25}Pd_xO_{2-\delta}$ ($x=0.01, 0.02$)	$Ce_{1-x-y}Zr_xPd_yO_{2-\delta}$ ($x=0.25, y=0.02$)	$Ce_{0.78}Sn_{0.2}Pd_{0.02}O_{2-\delta}$
Rh^{3+}	$Ce_{1-x}Rh_xO_{2-\delta}$ ($x=0.005, 0.01$)	$Ti_{1-x}Rh_xO_{2-\delta}$ ($x=0.01$)			
Pt^{2+}	$Ce_{1-x}Pt_xO_{2-\delta}$ ($x=0.01, 0.02$)	$Ti_{1-x}Pt_xO_{2-\delta}$ ($x=0.01$)	$Ce_{0.85-x}Ti_{0.15}Pt_xO_{2-\delta}$ ($x=0.01, 0.02$)		
Pt^{2+}, Rh^{3+}	$Ce_{1-x}Rh_{x/2}Pt_{x/2}O_{2-\delta}$ ($x=0.01, 0.02$)				

that at least 92 at.% of the platinum taken in the preparation of 1% Pt/CeO$_2$ is incorporated into CeO$_2$ lattice. Total oxygen content in 1% Pt/CeO$_2$ is 1.883 and that in pure CeO$_2$ is 1.934 and there is a decrease in lattice parameter in 1% Pt/CeO$_2$ compared to pure CeO$_2$. Similarly, diffraction lines due to Rh metal, Rh$_2$O$_3$ and RhO$_2$ were not detected in the XRD of 1% Rh/CeO$_2$ catalyst. Total oxygen content in 1% Rh/CeO$_2$ catalyst is 1.87, whereas it is 1.934 for pure CeO$_2$. Therefore, a decrease in oxygen content in the catalyst compared with pure CeO$_2$ signifies the creation of oxide ion vacancy. Thus, formation of solid solution phases of $Ce_{1-x}M_xO_{2-\delta}$ (M = Pd, Rh, Pt, Ru, Cu, Ag and Au) and $Ce_{1-x-y}Ti_yM_yO_{2-\delta}$ (M = Pd and Pt) have been ascertained from detailed XRD studies.[107–118] Similarly, solution combustion synthesized $Ti_{1-x}M_xO_2$ (M = Pd and Pt) catalysts crystallize in anatase structures.[119,120]

High resolution TEM (FeI Technai 20) image of all the catalysts shows cubic morphology of CeO$_2$ crystallites with average sizes of 25–30 nm. Noble metal particles are hardly observed on the crystallites. For example, a high resolution TEM image and electron diffraction pattern of combustion synthesized 2% Pd/Ce$_{0.75}$Ti$_{0.25}$O$_2$ is shown in Figure 3. The fringes spacing at ~3.12 Å corresponds to (111) layers of Ce$_{0.75}$Ti$_{0.25}$O$_2$. The electron diffraction pattern clearly shows fluorite structure of the compound and it is completely crystalline. There is no lattice fringe or ring due to Pd metal and fringes due to Pd metal particles separated at 2.25 Å are absent. On the other hand, Figure 3 C shows the ED pattern of 2% Pd/Ce$_{0.75}$Ti$_{0.25}$O$_2$ prepared by impregnation method and clearly Pd(111) ring is visible as indicated by arrow. Absence of diffraction ring due to Pd metal in the combustion synthesized material shows substitution of Pd in the lattice forming Ce$_{0.73}$Ti$_{0.25}$Pd$_{0.02}$O$_{2-\delta}$ solid solution.[118] The average particle size obtained from low magnification image is ~20 nm. Similarly,

Figure 3: TEM of Ce$_{0.73}$Ti$_{0.25}$Pd$_{0.02}$O$_{2-\delta}$ (A), electron diffraction of Ce$_{0.73}$Ti$_{0.25}$Pd$_{0.02}$O$_{2-\delta}$ (B) and Impregnated 2 at.% Pd/Ce$_{0.75}$Ti$_{0.25}$O$_2$ (C).
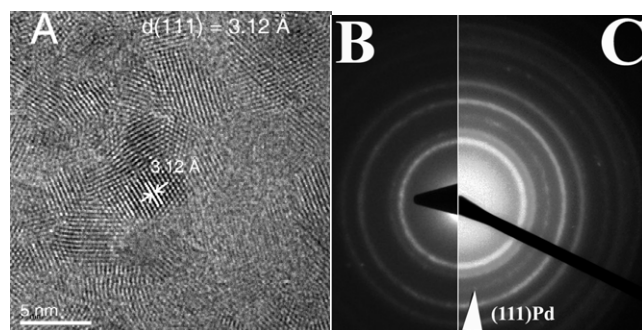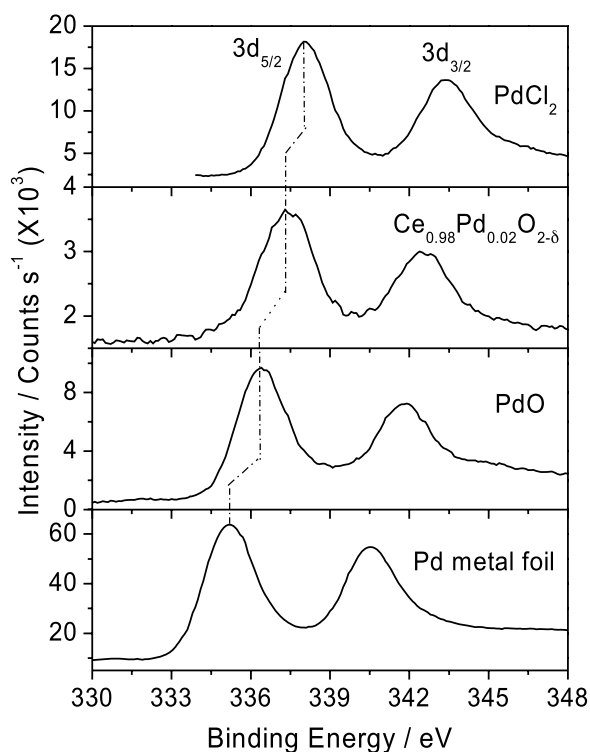
Figure 4: XPS of Pd metal, PdO, $Ce_{0.98}Pd_{0.02}O_{2-\delta}$ and $PdCl_2$.

a high resolution image of Pt ion substituted $Ce_{0.85}Ti_{0.15}O_2$ shows only 3.2 Å lattice fringes of (111) plane of $Ce_{0.85}Ti_{0.15}O_2$ and fringes due to Pt metal particles separated at 2.30 Å are absent. Energy dispersive X-xay spectroscopy (EDXS) from lattice fringes confirms the presence of 1% Pt in the catalyst. Therefore, absence of Pt metal fringes and presence of Pt X-ray emission confirmed Pt ion substitution in $Ce_{0.85}Ti_{0.15}O_2$.[117] In contrast, large number of nano size fine Pt metal particles can be dispersed on α-Al_2O_3 by solution combustion method.[109,121]

Oxidation states of Pt, Pd, Rh, Ru, Cu, Ag, Au, Ce and Ti present in the catalysts studied here could be obtained from XPS. For example, XPS (ESCA-3 Mark II, VG Scientific Ltd.) of Pd3d core level region of 2 at.% Pd/CeO_2 along with Pd metal, PdO and $PdCl_2$ is given in Figure 4. Pd$3d_{5/2}$ peaks are observed at 337.4, 335.2, 336.4 and 338.0 eV respectively for 2% Pd/CeO_2, Pd metal, PdO and $PdCl_2$. Thus, Pd core levels in 2% Pd/CeO_2 catalyst are shifted by 2.2 eV with respect to Pd metal, whereas Pd3d shift is 1.2 eV in comparison with PdO. Binding energies of Pd3d peaks in 2% Pd/CeO_2 are close to of Pd3d peaks in $PdCl_2$ clearly indicating that Pd^{2+} ions are much more ionic in CeO_2 matrix than PdO. XP spectrum of Ce3d with
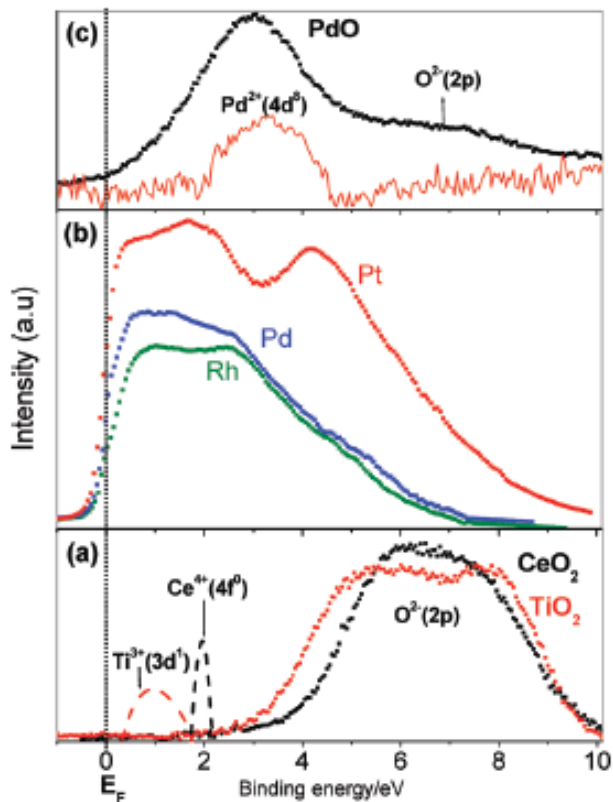
satellite features shows that Ce is present in +4 oxidation state in the catalyst. Therefore, XPS of 2% Pd/CeO_2 by combustion method clearly indicates that Pd is present in highly ionic Pd^{2+} state. In 1% Pt/CeO_2 catalyst, Pt is present in both +2 (85%) and +4 (15%) oxidation states.[109,110] Thus, XPS results demonstrate that Rh in $Ce_{1-x}Rh_xO_{2-\delta}$, Cu in $Ce_{1-x}Cu_xO_{2-\delta}$, Ag in $Ce_{1-x}Ag_xO_{2-\delta}$ and Au in $Ce_{1-x}Au_xO_{2-\delta}$ are fully dispersed in +3, +2, +1 and +3 oxidation states, respectively.[108,112–114]

Stabilization of noble metal ions in CeO_2 or TiO_2 could be substantiated from the relative positions of metal valence levels with respect to valence levels of CeO_2 and TiO_2. The valence band XPS of CeO_2 as well as TiO_2 consists of the O2p band spread over ∼3–9 eV (Figure 5a) and the empty Ce4f level is located at ∼2 eV below the Fermi level (E_F) where binding energy is referenced to zero. Pt, Pd, and Rh metals have high electron density at the E_F (Figure 5b) and the valence bands of these metals extend even up to 6 eV below E_F. When these metals are oxidized, M^{n+}d bands shift to higher binding energies with the effect that the M^{n+}d bands are located at about 2.5–3.5 eV below E_F as in PdO (Figure 5c). In $Ce_{1-x}M_xO_{2-\delta}$, the M^{n+}d band lies below the Ce4f level but above the O2p band and hence, Ce in the compound remains mostly in the +4 state. When metal ion in $Ce_{1-x}M_xO_{2-\delta}$ is reduced to metal in the lattice, the metal valence level moves up toward the E_F, which is above the empty Ce4f level. Hence, electron transfer from metal to Ce^{4+} ion ($M^0 + 2Ce^{4+}4f^0 \rightarrow M^{2+} + 2Ce^{3+}4f^1$) becomes facile and the noble metals remain ionic in CeO_2.[35] For example, the difference of valence band XPS of CeO_2 and $Ce_{0.98}Pd_{0.02}O_{1.98}$ shows a small density of states at ∼3.2 eV from E_F. This density of states corresponds to Pd^{2+}4d^8 occupied state that is higher than that of Ce4f level.[122] Similarly, Pt and Pd ions get stabilized in TiO_2 because Pt^{2+}5d and Pd^{2+}4d bands lie below Ti^{3+}3d and above O2p bands.

Substitution of metal ions into CeO_2 lattice has been confirmed by XAFS studies (SPring-8, Japan). XAFS analysis shows unique Ce–Pd and Ce–Rh and Ce–Pt distances at 3.31, 3.16 and 3.28 Å respectively, whereas Ce–Ce distance is observed at 3.84 Å demonstrating the metal ion substitution into CeO_2 lattice.[107,108,110] Significantly, these unique correlations are absent in either CeO_2 or noble metals or their oxides such as PtO_2, PdO and Rh_2O_3. Typical XAFS spectra of 1% Pd/CeO_2 along with PdO, Pd metal is shown in Figure 6. Lower coordination numbers around metal ions compared to Ce ion indicate the oxide ion vacancy due to lower valent metal ion substitution.

Based on the extensive characterization studies employing XRD, TEM, XPS and XAFS we have

Figure 5: Valence band XPS of (a) CeO_2 and TiO_2 (b) Pt, Pd, and Rh metals and (c) PdO and the difference of valence band spectra of $Ti_{0.99}Pd_{0.01}O_{1.99}$ and TiO_2 showing $Pd^{2+}4d$ band position.

doped CeO_2 compounds along with pure PdO and the corresponding oxides supports are shown in Figure 7. Pure CeO_2 shows H_2 uptake from 350 °C with a low temperature peak at ~500 °C, which has been attributed to surface cerium reduction followed by bulk cerium reduction beyond 550 °C. The area under the peak up to 700 °C corresponds to 5.2 cm^3 of H_2 per g of CeO_2. Reduction of Ti substituted compounds starts at 300 °C and $Ce_{0.75}Ti_{0.25}O_2$ is reduced to $Ce_{0.75}Ti_{0.25}O_{1.82}$. This composition corresponds to complete reduction of Ti^{4+} to Ti^{3+} and 8% of Ce^{4+} to Ce^{3+}. PdO is reduced at 80 °C and the area under the peak corresponds to PdO + $H_2 \rightarrow$ Pd + H_2O. A small negative peak after PdO reduction is attributed to the desorption of H_2 from the dissociation of PdH_x species. H_2 uptake starts at ~30 °C in $Ce_{0.98}Pd_{0.02}O_{2-\delta}$ with a hydrogen adsorption peak at ~65 °C and a small peak at 400 °C due to CeO_2 reduction is seen. Taking the low temperature H_2 peak at 65 °C, the ratio of H/Pd is four in $Ce_{0.98}Pd_{0.02}O_{2-\delta}$. In the case of $Ce_{0.73}Ti_{0.25}Pd_{0.02}O_{2-\delta}$, H/Pd ratio is 17. A ratio of H/Pd greater than 2 indicates reduction of support because, Pd^{2+} + 2 H can give Pd^0. Thus, $Ce_{0.75}Ti_{0.25}O_2$ upon substitution with Pd^{2+} ion is more easily reducible at temperature as low as 90 °C. The composition of the reduced oxide corresponds to $Ce_{0.73}Ti_{0.25}Pd_{0.02}O_{1.82}$ and it becomes $Ce_{0.73}Ti_{0.25}Pd_{0.02}O_{1.74}$ when reduced up to 700 °C. Thus there is a huge decrease in the reduction temperature of $Ce_{0.75}Ti_{0.25}O_2$ in

demonstrated that in combustion synthesized M/CeO_2 catalysts, metal ions are incorporated in the CeO_2 matrix in the form of solid solution phase $Ce_{1-x}M_xO_{2-\delta}$. In addition to the oxide ion vacancies created due to aliovalent ionic substitutions for Ce^{4+}, there seems to be additional oxide ion vacancies to the extent of 3.5% in nano CeO_2.

5.5. OSC of CeO_2 supported noble metal ion catalysts

To understand the reducibility of oxygen species as well as the metal–support interaction in CeO_2 and related materials, H_2-TPR is extensively employed where the volume of H_2 consumed by the reduction of an oxide is measured. Pure CeO_2, TiO_2, PdO, Rh_2O_3, CuO and SnO_2 show weak H_2 uptake peak at higher temperatures in comparison with metal substituted CeO_2. ZrO_2 does not show redox properties as there is no peak in their respective H_2-TPR profiles, whereas significant OSC have been observed in $Ce_{1-x}Zr_xO_2$ samples. For specific example, H_2-TPR profiles of CeO_2, Pd

Figure 6: XAFS of Pd metal, PdO and 1% Pd/CeO_2.
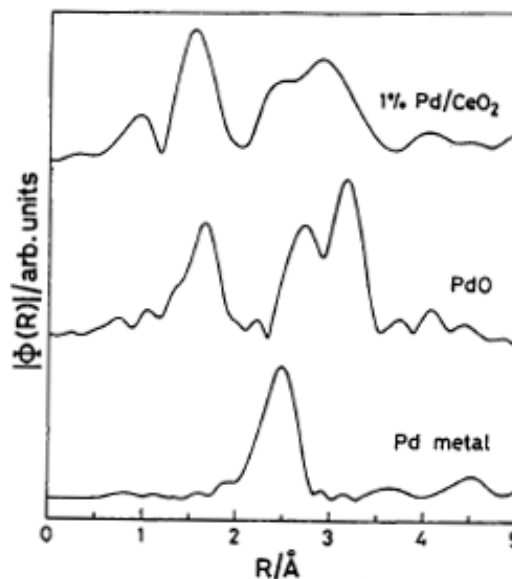
Figure 7: H₂-TPR of CeO_2, $Ce_{0.75}Ti_{0.25}O_2$, PdO, $Ce_{0.98}Pd_{0.02}O_{2-\delta}$ and $Ce_{0.73}Pd_{0.25}Pd_{0.02}O_{2-\delta}$.
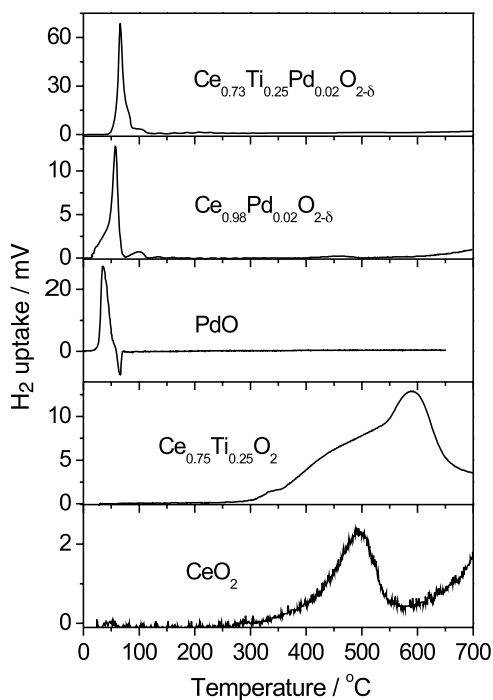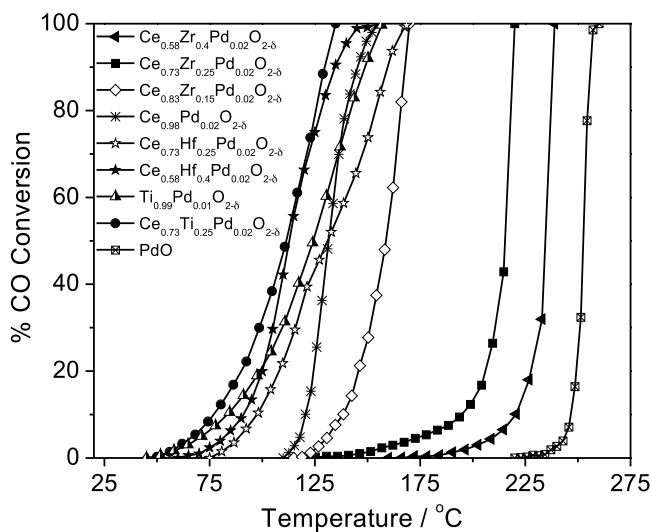

Figure 8: CO oxidation reaction over several combustion synthesized catalysts.

presence of 2% Pd ion in the lattice. Thus, Ti^{4+} to Ti^{3+} and Ce^{4+} to Ce^{3+} reduction temperature decreased in presence of Pd^{2+} ion. Similarly, not

only Rh^{3+} ion in $Ce_{1-x}Rh_xO_{2-\delta}$ gets reduced but part of Ce^{4+} ion also gets reduced with H/Rh > 4.8 for $Ce_{0.99}Rh_{0.01}O_{2-\delta}$ and the process is reversible. In $Ce_{1-x}Ti_xO_2$, the oxide ions are already activated due to distortion of oxide ion sublattice. Pt or Pd ionic substitution in the mixed oxide further activates the lattice oxygen. In fact, hydrogen is adsorbed at room temperature over Pt or Pd ion doped $Ce_{1-x}Ti_xO_2$ with H/Pt and H/Pd ratios of ~10 and ~15, respectively. Oxygen storage capacities of a large number of CeO_2 based materials studied in our laboratory are given in Table 7.[108,111,115−118,122−126]

From our studies with H₂-TPR, XAFS, DFT calculations, it has been found that change of structure at the atomic level is to be the reason for higher OSC in these types of mixed oxides. Because of the smaller size of substituent cation, surrounding oxygen ions are displaced from the original position and the oxygens at a larger distance are removed by reducing gas easily. In $Ce_{1-x}Zr_xO_2$, there are several long and short Ce–O and Zr–O bonds compared to pure CeO_2 and ZrO_2. Short bonds are strong, whereas long bonds are weak that could be easily removed by H₂ leading to higher OSC.[116] Similarly, XAFS studies and DFT calculations show the presence of short and long Ce–O and Ti–O bonds $Ce_{1-x}Ti_xO_2$ which gives strong and weakly bound oxygens.[115] The stronger bonds have a valency greater than 2 and the weaker ones have a valency less than 2 and weakly bound oxygen has been found to be responsible for higher OSC in these mixed oxides. On the other hand, this kind of situation could not be found out in pure CeO_2 and TiO_2, thereby these pure oxides show lower OSC compared to mixed oxides.

5.6. Exhaust catalysis on CeO_2 supported metal ion catalysts

The noble metal ionic catalysts were examined for various catalytic reactions and their activities were compared with the corresponding metals supported on oxides. Among the noble Pt, Pd, and Rh metal ions, Pd ion substituted CeO_2 or $Ce_{1-x}Ti_xO_2$ or TiO_2 showed the highest rate of CO conversion and lowest activation energy towards CO oxidation. In this sense, it would be noteworthy that Pd is the cheapest among noble metals. A typical %CO conversion profile for CO oxidation reaction over Pd substituted catalysts are shown in Figure 8. It has also been also that activation energy decreases with increase in the effective charge on Pd ion in these oxides.[123] There are also points to note that in general, rates with metal ionic catalysts are higher by 20–30 times compared with the same amount of metal impregnated catalysts.

Table 7: Oxygen storage capacities (OSC) of CeO_2 based materials studied in our laboratory.

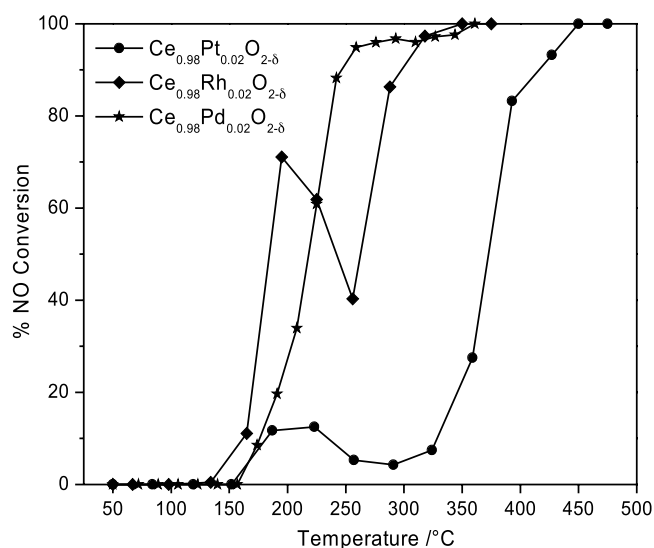| Materials	Composition after reduction	OSC (μmol g^{-1})	References
CeO_2	$CeO_{1.97}$	174	123
$Ce_{0.98}Rh_{0.02}O_{1.99}$	$Ce_{0.98}Rh_{0.02}O_{1.95}$	244	108
$Ce_{0.8}Zr_{0.2}O_2$	$Ce_{0.8}Zr_{0.2}O_{1.81}$	1130	122
$Ce_{0.75}Zr_{0.25}O_2$	$Ce_{0.75}Zr_{0.25}O_{1.7}$	1900	116
$Ce_{0.6}Zr_{0.4}O_2$	$Ce_{0.6}Zr_{0.4}O_{1.63}$	2429	123
$Ce_{0.5}Zr_{0.5}O_2$	$Ce_{0.5}Zr_{0.5}O_{1.57}$	2900	116
TiO_2	$TiO_{1.92}$	1000	117
$Ce_{0.9}Ti_{0.1}O_2$	$Ce_{0.9}Ti_{0.1}O_{1.88}$	740	117
$Ce_{0.85}Ti_{0.15}O_2$	$Ce_{0.85}Ti_{0.15}O_{1.86}$	880	117
$Ce_{0.8}Ti_{0.2}O_2$	$Ce_{0.8}Ti_{0.2}O_{1.83}$	1110	117
$Ce_{0.75}Ti_{0.25}O_2$	$Ce_{0.75}Ti_{0.25}O_{1.81}$	1340	115
$Ce_{0.7}Ti_{0.3}O_2$	$Ce_{0.7}Ti_{0.3}O_{1.77}$	1590	117
$Ce_{0.6}Ti_{0.4}O_2$	$Ce_{0.6}Ti_{0.4}O_{1.73}$	2000	117
$Ce_{0.99}Pt_{0.01}O_{1.99}$	$Ce_{0.99}Pt_{0.01}O_{1.95}$	290	117
$Ce_{0.84}Ti_{0.15}Pt_{0.01}O_{1.99}$	$Ce_{0.84}Ti_{0.15}Pt_{0.01}O_{1.75}$	1570	117
$Ce_{0.83}Ti_{0.15}Pt_{0.02}O_{1.98}$	$Ce_{0.83}Ti_{0.15}Pt_{0.02}O_{1.63}$	2320	117
$Ce_{0.73}Ti_{0.25}Pd_{0.02}O_{1.98}$	$Ce_{0.73}Ti_{0.25}Pd_{0.02}O_{1.79}$	1286	123
$Ce_{0.75}Hf_{0.25}O_2$	$Ce_{0.75}Hf_{0.25}O_{1.87}$	714	123
$Ce_{0.73}Hf_{0.25}Pd_{0.02}O_{1.98}$	$Ce_{0.73}Hf_{0.25}Pd_{0.02}O_{1.78}$	1121	123
$Ce_{0.58}Hf_{0.4}Pd_{0.02}O_{1.98}$	$Ce_{0.58}Hf_{0.4}Pd_{0.02}O_{1.83}$	804	123
$Ce_{0.98}Pd_{0.02}O_{1.98}$	$Ce_{0.98}Pd_{0.02}O_{1.94}$	232	123
$Ce_{0.83}Zr_{0.15}Pd_{0.02}O_{1.98}$	$Ce_{0.83}Zr_{0.15}Pd_{0.02}O_{1.87}$	638	123
$Ce_{0.73}Zr_{0.25}Pd_{0.02}O_{1.98}$	$Ce_{0.73}Zr_{0.25}Pd_{0.02}O_{1.74}$	1509	123
$Ce_{0.58}Zr_{0.4}Pd_{0.02}O_{1.98}$	$Ce_{0.58}Zr_{0.4}Pd_{0.02}O_{1.73}$	1612	123
$Ce_{0.9}Sn_{0.1}O_2$	$Ce_{0.9}Sn_{0.1}O_{1.83}$	980	124
$Ce_{0.8}Sn_{0.2}O_2$	$Ce_{0.8}Sn_{0.2}O_{1.72}$	1650	124
$Ce_{0.7}Sn_{0.3}O_2$	$Ce_{0.7}Sn_{0.3}O_{1.63}$	2100	124
$Ce_{0.6}Sn_{0.4}O_2$	$Ce_{0.6}Sn_{0.4}O_{1.58}$	2545	124
$Ce_{0.5}Sn_{0.5}O_2$	$Ce_{0.5}Sn_{0.5}O_{1.56}$	2780	124
$Ce_{0.78}Sn_{0.2}Pd_{0.02}O_{1.98}$	$Ce_{0.78}Sn_{0.2}Pd_{0.02}O_{1.7}$	1650	122
$Ce_{0.5}Sn_{0.48}Pd_{0.02}O_{1.98}$	$Ce_{0.5}Sn_{0.48}Pd_{0.02}O_{1.77}$	1330	122
$Ce_{0.78}Zr_{0.2}Pd_{0.02}O_{1.98}$	$Ce_{0.78}Zr_{0.2}Pd_{0.02}O_{1.88}$	620	122
$Ce_{0.95}Ru_{0.05}O_{1.97}$	$Ce_{0.95}Ru_{0.05}O_{1.75}$	1335	111
$Ce_{0.9}Ru_{0.1}O_{1.94}$	$Ce_{0.9}Ru_{0.1}O_{1.52}$	2513	111
$Ce_{0.9}Fe_{0.1}O_{1.88}$	$Ce_{0.9}Fe_{0.1}O_{1.77}$	665	125
$Ce_{0.89}Fe_{0.1}Pd_{0.01}O_{1.84}$	$Ce_{0.89}Fe_{0.1}Pd_{0.01}O_{1.71}$	780	125
$Ce_{0.67}Cr_{0.33}O_{2.11}$	$Ce_{0.67}Cr_{0.33}O_{1.75}$	2513	126

Pd substituted $Ce_{1-x}Sn_xO_2$ and $Ce_{1-x}Fe_xO_2$ also shows high OSC as well as CO conversion.[122,124] CO conversion rates for $CO + O_2$ reaction over several catalysts studied in our laboratory are at least one order magnitude higher than catalysts reported in the literature (Table 8).[127–131] In another type of experiment, CO gets oxidized to CO_2 by extracting activated lattice oxygen in the absence of feed oxygen. On exposure to oxygen, the lattice oxygen is replenished. This means that the feed oxygen gets adsorbed and incorporated in the oxide ion vacancy indicating the presence of two independent sites on the catalyst that adsorb reducing and oxidizing molecules respectively.[111,118,124]

$Ce_{0.98}Pd_{0.02}O_{2-\delta}$ shows high rates of NO and N_2O reduction by CO compared with Pt, Pd, and Rh metal supported catalysts. N_2 selectivity is highest among all the three catalysts in the entire temperature range. In the temperature range of 125–350 °C, N_2 selectivity is more than 70% over $Ce_{0.98}Pd_{0.02}O_{2-\delta}$, whereas at the same temperature range N_2 selectivity is only 40–50% with $Ce_{0.98}Rh_{0.02}O_{2-\delta}$ catalyst and it is much less ($\sim$20%) with $Ce_{0.98}Pt_{0.02}O_{2-\delta}$. But N_2 selectivities are more or less same over all catalyst at higher temperature ($>$300 °C).[132,133] A comparison of Pt, Pd and Rh ion substituted CeO_2 showed higher catalytic activity with Pd ion than both Pt and Rh ions (Figure 9). $Ti_{0.99}Pd_{0.01}O_{1.99}$ also shows high rates of NO conversion and high N_2 selectivity and specifically, rates of N_2O reduction by CO are very high.[134] NO conversion rates and N_2 selectivities for NO + CO reaction over several catalysts studied in our laboratory are much higher than the catalysts reported in the literature (Table 9).[135–140] More than three hydrogen adsorptions per Pd^{2+} ion

Table 8: Comparison of CO conversion rates and activation energies (E_a) for CO + O_2 reaction over several reported catalysts.

Catalysts	Rate (μmol g^{-1} s^{-1})	E_a (kJ mol^{-1})	References
5 wt.% Ru/SiO$_2$	1.0 (110 °C)	94	127
5 wt.% Rh/SiO$_2$	0.0251 (110 °C)	103	127
5 wt.% Pd/SiO$_2$	0.316 (143 °C)	103	127
5 wt.% Ir/SiO$_2$	0.26 (180 °C)	105	127
5 wt.% Pt/SiO$_2$	0.32 (115 °C)	56	127
Pd/CeO$_2$/Al$_2$O$_3$	38.0 (250 °C)	84	128
0.014 wt.% Rh/Al$_2$O$_3$	0.6 (196 °C)	115.5	129
0.014 wt.% Rh/9 wt.% Ce/Al$_2$O$_3$	0.95 (196 °C)	90.3	129
0.5 wt.% Pd/CeO$_2$−ZrO$_2$	0.7 (220 °C)	175	130
Pd/SiO$_2$	0.155 (140 °C)	-	131
25Au75Pd/SiO$_2$	0.128 (140 °C)	-	131
50Au50Pd/SiO$_2$	0.06 (140 °C)	-	131
Ce$_{0.98}$Pd$_{0.02}$O$_{2-\delta}$	7.0 (130 °C)	67.2	Our work (118)
1 at.% Pd/Al$_2$O$_3$ (Impregnated)	2.73 (200 °C)	86.88	Our work (134)
1 at.% Pd/TiO$_2$ (Impregnated)	0.758 (100 °C)	75.25	Our work (134)
Ce$_{0.99}$Pt$_{0.01}$O$_{2-\delta}$	0.6 (155 °C)	55.4	Our work (117)
Ce$_{0.84}$Ti$_{0.15}$Pt$_{0.01}$O$_{2-\delta}$	28.0 (155 °C)	82.3	Our work (117)
Ce$_{0.73}$Ti$_{0.25}$Pd$_{0.02}$O$_{2-\delta}$	18.0 (120 °C)	54.6	Our work (118)
2% Pd/Ce$_{0.75}$Ti$_{0.25}$O$_{2-\delta}$	-	132.3	Our work (118)
Ce$_{0.78}$Sn$_{0.2}$Pd$_{0.02}$O$_{2-\delta}$	1.9 (50 °C)	84	Our work (124)
Ce$_{0.95}$Ru$_{0.05}$O$_{2-\delta}$	2.05 (100 °C)	94.5	Our work (111)
Ce$_{0.9}$Ru$_{0.1}$O$_{2-\delta}$	3.3 (100 °C)	44.8	Our work (111)
Ce$_{0.89}$Fe$_{0.1}$Pd$_{0.01}$O$_{2-\delta}$	-	52.5	Our work (125)
Ce$_{0.9}$Fe$_{0.1}$O$_{2-\delta}$	-	46.2	Our work (125)
Ce$_{0.99}$Pd$_{0.01}$O$_{2-\delta}$	-	63	Our work (125)

Figure 9: NO + CO reaction over Pt, Pd and Rh doped CeO$_2$.

Pd, Rh and Ru) have been studied and again, Pd ion is found to be better than other noble metal ions.[120] High rates of NO to N$_2$ conversion were observed over the Pd^{2+} ion substituted CeO$_2$ catalyst during SCR in presence of excess oxygen. On Ce$_{0.73}$Ti$_{0.25}$Pd$_{0.02}$O$_{2-\delta}$, NO conversion rates and N$_2$ selectivity are higher than on Ce$_{0.98}$Pd$_{0.02}$O$_{2-\delta}$. SCR of NO by NH$_3$ over Ti$_{1-x}$M$_x$O$_{2-\delta}$ (M = Cr, Mn, Fe, Co or Cu; $x = 0.1$) shows high selectivity with Fe ion.[142] With noble metal ions in TiO$_2$, dissociation rate of NH$_3$ is low, while Mn or Fe ion in TiO$_2$ shows higher dissociation.[143]

5.7. Reaction mechanism on metal ion doped CeO$_2$ catalysts

Earlier we have demonstrated that there are two independent sites on the metal ionic catalyst which adsorb reducing and oxidizing molecules, respectively during redox type of reactions. A dual site mechanism of CO oxidation based on the structure of Ce$_{1-x}$Pt$_x$O$_{2-\delta}$ is compared with Langmuir–Hinshelwood mechanism on Pt metal surface in Figure 10. Dissociation of oxygen occurs due to the expansion of O–O bond over Pt metal surface. On the Pt ionic catalyst surface, CO is adsorbed on the electron-deficient metal ions, whereas O$_2$ is adsorbed on the oxide ion vacancy

in Ce$_{1-x}$Pd$_x$O$_{2-\delta}$ makes it a better catalyst for NO reduction by H$_2$ and 100% N$_2$ selectivity is observed at low temperature.[141] NO and N$_2$O reduction by H$_2$ over Ti$_{0.99}$M$_{0.01}$O$_{2-\delta}$ (M = Pt,

Table 9: Comparison of NO conversion rates, activation energies (E_a) and nitrogen selectivities (S_{N_2}) for NO + CO reaction over several reported catalysts.

Catalysts	Rate (μmol g^{-1} s^{-1})	E_a (kJ mol^{-1})	S_{N_2}	S_{N_2O}	References
1 wt.% Pt/Al$_2$O$_3$	0.1 (300 °C)	92.4	27	73	135
0.2 wt.% Rh/Al$_2$O$_3$	7.2 (300 °C)	184.8	32	68	136
1 wt.% Pt-0.02 wt.% Rh/Al$_2$O$_3$	0.58 (300 °C)	126	39	61	136
Pt-Rh/Al$_2$O$_3$-CeO$_2$	0.54 (300 °C)	84	33	67	137
Rh/Al$_2$O$_3$	0.58 (227 °C)	86.6	45	55	138
Pd/Rh/Al$_2$O$_3$	0.11 (227 °C)	100	43	57	138
Pd/Al$_2$O$_3$	0.83 (227 °C)	59.8	36	64	138
Pd/La$_2$O$_3$/Al$_2$O$_3$	4.3 (227 °C)	100	30	70	138
1% Pd/γ-Al$_2$O$_3$	0.75 (287 °C)	158	34	66	139
Pd8Mo/Al$_2$O$_3$	2.0 (300 °C)	84	39	61	140
Ce$_{0.98}$Pd$_{0.02}$O$_{2-\delta}$	0.242 (175 °C)	70.2	75	25	Our work (132)
	1.51 (200 °C)		81	19	
	2.67 (225 °C)		77	23	
Ti$_{0.99}$Pd$_{0.01}$O$_{2-\delta}$	1.47 (175 °C)	64.13	70	30	Our work (134)
	3.09 (200 °C)		51	49	
	5.13 (225 °C)		62	38	
1% Pd/Al$_2$O$_3$ (Impregnated)	0.05 (240 °C)	86.6	59	41	Our work (132)
Ce$_{0.99}$Pt$_{0.01}$O$_{2-\delta}$	0.2 (135 °C)	100.8	-	-	Our work (117)
Ce$_{0.84}$Ti$_{0.15}$Pt$_{0.01}$O$_{2-\delta}$	0.2 (135 °C)	96.6	-	-	Our work (117)
Ce$_{0.73}$Ti$_{0.25}$Pd$_{0.02}$O$_{2-\delta}$	2.0 (180 °C)	52.9	-	-	Our work (118)
Ce$_{0.78}$Sn$_{0.2}$Pd$_{0.02}$O$_{2-\delta}$	5.0 (150 °C)	105.4	100	-	Our work (124)
Ce$_{0.95}$Ru$_{0.05}$O$_{2-\delta}$	3.8 (200 °C)	41	100	-	Our work (111)
Ce$_{0.9}$Ru$_{0.1}$O$_{2-\delta}$	3.4 (200 °C)	53.2	100	-	Our work (111)

because the vacancy site is activated by the electron-rich environment. The size of the oxide ion vacancy is $\sim$2.8 Å, which can accommodate the oxygen molecule of diameter 2.42 Å. Thus, there are two distinct sites, one for reducing and another for oxidizing molecules, in the ionic catalysts unlike Pt metal. Electron transfer from reducing molecules to oxygen is facilitated by the lattice via coupling between accessible Pt^{2+}/Pt^0 and Ce^{4+}/Ce^{3+} redox couples. The enhanced activity is due to the creation of redox sites leading to site-specific adsorption and electronic interaction between the noble metal ions and the lattice. In addition to this, the lattice oxygen is activated in the catalyst with long M–O and Ce–O bonds and CO can get oxidized through a Mars–van Krevelen mechanism whereby oxide ion is continuously consumed and formed. The difference in the rate of CO oxidation over different metal ion substituted catalysts should be due to differences in their redox properties. Similar explanation could be given for NO + CO reaction. NO is an electron donor as well as an acceptor molecule. Therefore, on the ionic catalysts depicted in Figure 10, NO can be molecularly adsorbed on noble metal ions and dissociatively chemisorbed on the oxide ion vacant sites. CO is specifically adsorbed on metal ion sites. NO adsorbed molecularly on the metal ion sites would lead to N$_2$O formation and on the oxide ion vacant site to N$_2$ formation.

5.8. Exhaust catalysis with CeO$_2$ based metal ion catalysts coated on cordierite monolith

In recent days, monolith supports are attractive alternative carriers for catalysts in heterogeneous catalysis. Monolith supports could either be metallic or ceramic containing single blocks of small (0.5–4 mm) parallel channels with catalytic wall and the structure looks like honeycomb. The monolith could be thought of as a series of parallel tubes with a cell density ranging from 300 to 1200 cpsi. At present, monoliths have been extensively used as catalyst supports inside the catalytic converters for exhaust gas clean up in the automobile industry.[30–32,144–146] Generally, a catalyst is coated on a ceramic monolith support of honeycomb structure. Monolith is first coated with high surface area oxide like γ-Al$_2$O$_3$ and the process is called washcoating. After washcoating, catalyst active phase is dispersed over the monolith support. There are several methods for washcoating and coating of catalyst active phase on monoliths which has been described in several articles.[147,148] Monolithic support dominates the entire automotive market as the preferred catalyst support due to advances in monolith technology, simple catalyst mounting methods, flexibility in reactor design, low pressure drop and high heat and mass transfer rates. Among monolith supports ceramic monolith materials are leaders in the market and the preferred material is cordierite.
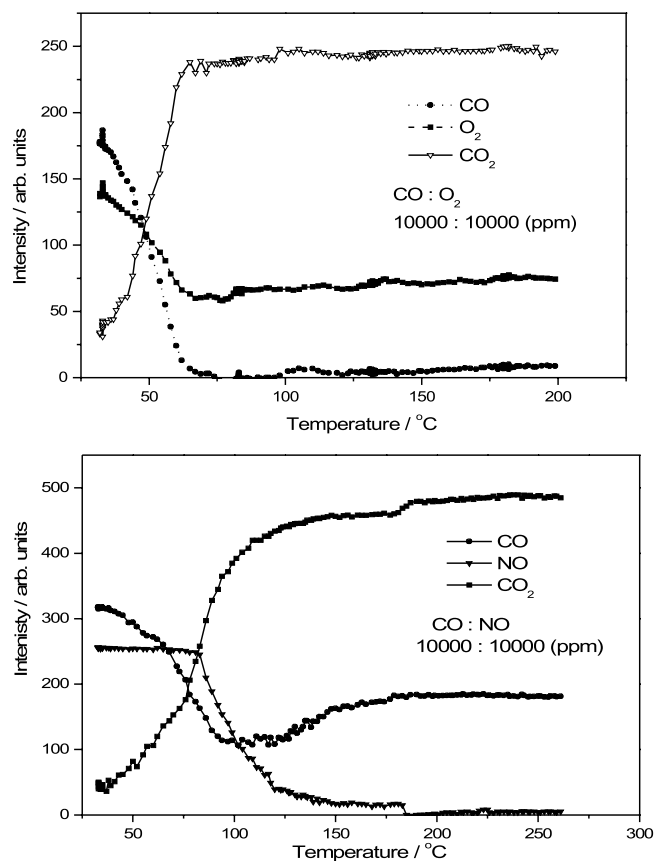
Figure 10: (a) Langmuir–Hinshelwood mechanism of CO + O$_2$ reaction on Pt metal surface and (b) mechanism of CO + O$_2$ reaction on Ce$_{1-x}$Pt$_x$O$_{2-\delta}$.
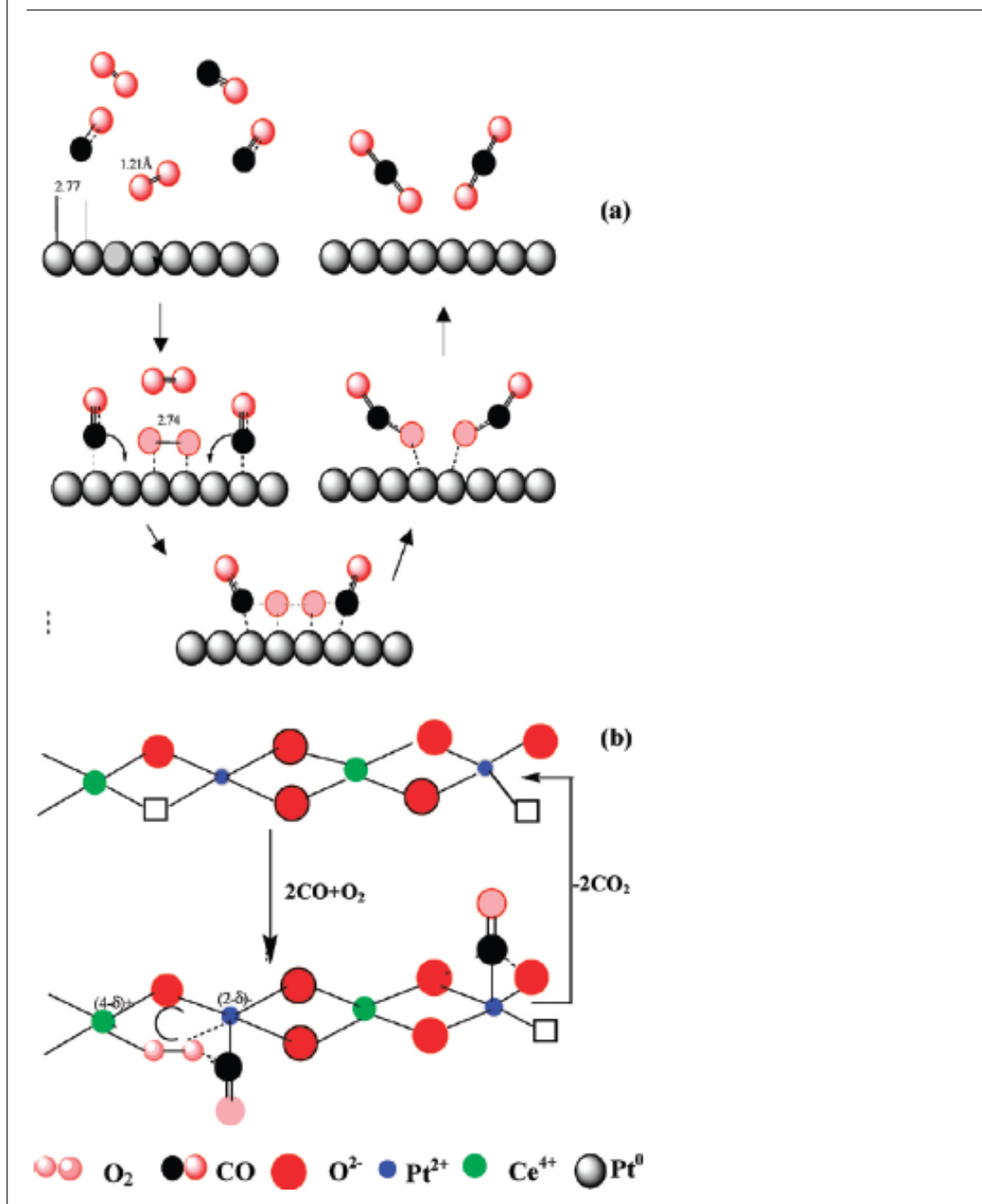
In order to examine the reactivity for exhaust catalysis over ionic catalysts supported on ceramic monolith, these catalysts are coated on cordierite honeycombs by a single-step combustion method. The process consists of growing γ-Al$_2$O$_3$ on cordierite by solution combustion method and active catalyst phase, Ce$_{0.98}$Pd$_{0.02}$O$_{2-\delta}$ on γ-Al$_2$O$_3$ coated cordierite again by the same method. About 100% conversion of CO is achieved below 80 °C at a space velocity of 880 h^{-1}. At much higher space velocity of 21,000 h^{-1}, 100% conversion is obtained below 245 °C.[149, 150] At a space velocity of 880 h^{-1}, 100% NO conversion is attained below 185 °C and 100% conversion of HC (C$_2$H$_2$) below 220 °C. Typical CO + O$_2$ and NO + CO reactions over Ce$_{0.98}$Pd$_{0.02}$O$_{2-\delta}$ coated on cordierite monolith are given in Figure 11. At same space velocity three-way catalytic performance over Ce$_{0.98}$Pd$_{0.02}$O$_{2-\delta}$ coated monolith shows 100% conversion of all the pollutants below 220 °C with 15% of excess oxygen.

Figure 11: $CO + O_2$ and $NO + CO$ reactions over $Ce_{0.98}Pd_{0.02}O_{2-\delta}$ coated on cordierite monolith.

catalytic reactions such as CO and hydrocarbon oxidation and NO reduction by CO, NH_3 and H_2. This special preparation technique for dispersing ionic metals could be extended to the other reducible transition metal oxide supports such as SnO_2, V_2O_5, WO_3 and MoO_3 and these materials could be probed for several reactions related to auto exhaust catalysis exploring more insights into the metal–support interaction, redox properties and synergistic effects.

In last 30 years, pollutions from automotive exhaust are a major concern for our environment and numerous studies are being carried out to abate the pollutants through catalysis. We hope, ionically dispersed noble metal catalysts synthesized by solution combustion method could provide a new direction to achieve best performing catalysts for several abatement reactions for auto exhaust clean up. In broad sense, extensive studies on these materials for several heterogeneous catalytic reactions of present-days' importance other than auto exhaust catalytic reactions would be worthwhile area to carry out in catalysis coupled with solid state chemistry view point.

Acknowledgments

References

1. R. S. Yolles, H. Wise and S. W. Weller, *Crit. Rev. Environ. Sci. Technol.*, **2**, 125 (1971).
2. F. G. Dwyer, *Catal. Rev.*, **6**, 261 (1972).
3. M. Shelef, *Catal. Rev.*, **11**, 1 (1975).
4. J. T. Kummer, *Prog. Energy Combust. Sci.*, **6**, 177 (1980).
5. K. C. Taylor, in *Catalysis: Science and Technology*, Volume 5, Chapter 2, Eds.: J. R. Anderson and M. Boudart, Springer-Verlag, Berlin, 1984.
6. H. Bosch and F. Janssen, *Catal. Today*, **2**, 369 (1988).
7. P. N. Hawker, *Sci. Total Environ.*, **93**, 231 (1990).
8. J. N. Armor, *Appl. Catal. B*, **1**, 221 (1992).
9. J. N. Armor, *Chem. Mater.*, **6**, 730 (1994).
10. M. Shelef, *Chem. Rev.*, **95**, 209 (1995).
11. M. D. Amiridis, T. Zhang and R. J. Farrauto, *Appl. Catal. B*, **10**, 203 (1996).
12. F. J. Janssen in *Handbook of Heterogeneous Catalysis*, Volume 4, Eds.: G. Ertl, H. Knözinger and J. Weitkamp, Wiley-VCH, Weinheim, 1997, p. 1633.
13. G. C. Koltsakis and A. M. Stamatelos, *Prog. Energy Combust. Sci.*, **23**, 1 (1997).
14. A. Fritz and V. Pitchon, *Appl. Catal. B*, **13**, 1 (1997).
15. S. Matsumoto, *Catal. Surv. Jpn.*, **1**, 111 (1997).
16. V. I. Pârvulescu, P. Grange and B. Delmon, *Catal. Today*, **46**, 233 (1998).
17. G. Busca, L. Lietti, G. Ramis and F. Berti, *Appl. Catal. B*, **18**, 1 (1998).
18. B. E. Nieuwenhuys, *Adv. Catal.*, **44**, 259 (1999).

Thus, Pd^{2+} incorporated CeO_2 catalyst coated on cordierite shows significant activity toward the reactions related to auto exhaust catalysis.

6. Conclusions and future directions

A new approach of dispersing metal ions over CeO_2 and TiO_2 by solution combustion technique resulting in $Ce_{1-x}M_xO_{2-\delta}$ and $Ti_{1-x}M_xO_{2-\delta}$ (M = Pd, Rh and Pt) catalysts, structure of these materials and their catalytic properties are documented here. As the solution combustion method is a redox reaction type of preparation procedure, in these materials, noble metal ions are incorporated to a certain limit into the reducible oxide substrate matrices like CeO_2 and TiO_2. In this point of view, this preparation method for the supported metal catalysts is unique and different from other conventional techniques. Extensive works done in the last 10 years in our laboratory have established that these ionically dispersed metal catalysts show very high OSC and they are catalytically much more active than usual dispersed fine metal particles toward several auto exhaust

19. S. Bhattacharyya and R. K. Das, *Int. J. Energy Res.*, **23**, 351 (1999).
20. R. J. Farrauto and R. M. Heck, *Catal. Today*, **55**, 179 (2000).
21. M. Shelef and R. W. McCabe, *Catal. Today*, **62**, 35 (2000).
22. R. M. Heck and R. J. Farrauto, *Appl. Catal. A*, **221**, 443 (2001).
23. J. Kašpar, P. Fornasiero and N. Hickey, *Catal. Today*, **77**, 419 (2003).
24. H. S. Gandhi, G. W. Graham and R. W. McCabe, *J. Catal.*, **216**, 433 (2003).
25. F. Klingstedt, K. Arve, K. Eränen and D. Yu. Murzin, *Acc. Chem. Res.*, **39**, 273 (2006).
26. E. S. J. Lox, in *Handbook of Heterogeneous Catalysis*, 2nd Edition, Volume 5, Eds.: G. Ertl, H. Knözinger, F. Schüth and J. Weitkamp, Wiley-VCH, Weinheim, 2008, p. 2274.
27. P. Gabrielsson and H. G. Pedersen, in *Handbook of Heterogeneous Catalysis*, 2nd Edition, Volume 5, Eds.: G. Ertl, H. Knözinger, F. Schüth and J. Weitkamp, Wiley-VCH, Weinheim, 2008, p. 2345.
28. M. Bowker, *Chem. Soc. Rev.*, **37**, 2204 (2008).
29. M. V. Twigg, *Platinum Met. Rev.*, **47**, 157 (2003).
30. M. V. Twigg, *Phil. Trans. R. Soc. A*, **363**, 1013 (2005).
31. M. V. Twigg, *Catal. Today*, **117**, 407 (2006).
32. M. V. Twigg, *Appl. Catal. B*, **70**, 2 (2007).
33. S. Roy and A. Baiker, *Chem. Rev.*, **109**, 4054 (2009).
34. S. Roy, M. S. Hegde and G. Madras, *Appl. Energy*, **86**, 2283 (2009).
35. M. S. Hegde, K. C. Patil and G. Madras, *Acc. Chem. Res.*, **42**, 704 (2009).
36. J. N. Galloway, F. J. Dentener, E. Marmer, Z. Cai, Y. P. Abrol, V. K. Dadhwal and A. V. Murugan, *Annu. Rev. Environ. Resour.*, **33**, 461 (2008).
37. R. G. Prinn, *Annu. Rev. Environ. Resour.*, **28**, 29 (2003).
38. L. J. Muzio and G. C. Quartucy, *Prog. Energy Combust. Sci.*, **23**, 233 (1997).
39. http://www.epa.gov/air/emissions/nox.htm
40. J. H. Seinfeld, *Science*, **243**, 745 (1989).
41. Y. Qin, G. S. Tonnesen and Z. Wang, *Atmos. Environ.*, **38**, 3069 (2004).
42. D. Pudasainee, B. Sapkota, M. L. Shrestha, A. Kaga, A. Kondo and Y. Inoue, *Atmos. Environ.*, **40**, 8081 (2006).
43. P. J. Crutzen, *Angew. Chem. Int. Ed. Engl.*, **35**, 1758 (1996).
44. M. J. Molina, *Angew. Chem. Int. Ed. Engl.*, **35**, 1778 (1996).
45. F. S. Rowland, *Angew. Chem. Int. Ed. Engl.*, **35**, 1786 (1996).
46. F. S. Rowland, *Phil. Trans. R. Soc. B*, **361**, 769 (2006).
47. A. J. Haagen-Smit, *Ind. Eng. Chem.*, **44**, 1342 (1952).
48. P. L. Magill and R. W. Benoliel, *Ind. Eng. Chem.*, **44**, 1347 (1952).
49. A. J. Haagen-Smit and M. M. Fox, *Ind. Eng. Chem.*, **48**, 1484 (1956).
50. F. E. Littman, H. W. Ford and N. Endow, *Ind. Eng. Chem.*, **48**, 1492 (1956).
51. E. R. Stephens, P. L. Hanst, R. C. Doerr and W. E. Scott, *Ind. Eng. Chem.*, **48**, 1498 (1956).
52. M. S. Bergin, J. J. West, T. J. Keating and A. G. Russell, *Annu. Rev. Environ. Resour.*, **30**, 1 (2005).
53. http://en.wikipedia.org/wiki/ United_States_emission_standards.
54. http://en.wikipedia.org/wiki/ European_emission_standards
55. K. He, H. Huo and Q. Zhang, *Annu. Rev. Environ. Resour.*, **27**, 397 (2002).
56. http://en.wikipedia.org/wiki/Emission_standard
57. R. J. Farrauto and R. M. Heck, *Catal. Today*, **51**, 351 (1999).
58. Y. Teraoka and S. Kagawa, *Catal. Surv. Jpn.*, **2**, 155 (1998).
59. P. Zelenka, W. Cartellieri and P. Herzog, *Appl. Catal. B*, **10**, 3 (1996).
60. A. P. Walker, *Top. Catal.*, **28**, 165 (2004).
61. J. Suzuki and S. Matsumoto, *Top. Catal.*, **28**, 171 (2004).
62. T. Hu, Y. Wei, S. Liu and L. Zhou, *Energy Fuels*, **21**, 171 (2007).
63. M. Weilenmann, P. Soltic, C. Saxer, A.-M. Forss and N. Heeb, *Atmos. Environ.*, **39**, 2433 (2005).
64. G. E. Andrews, H. Li, J. A. Wylie, G. Zhu, M. Bell and J. Tate, *SAE*, 011617 (2005).
65. D. Ludykar, R. Westerholm and J. Almén, *Sci. Total Environ.*, **235**, 65 (1999).
66. M. J. Heimrich, S. Albu and M. Ahuja, *J. Eng. Gas Turbines Power*, **114**, 496 (1992).
67. P. A. Konstantinidis, G. C. Koltsakis and A. M. Stamatelos, *Proc. Inst. Mech. Eng. Part D: J. Automob. Eng.*, **211**, 21 (1997).
68. G. N. Coppage and S. R. Bell, *J. Eng. Gas Turbines Power*, **123**, 125 (2001).
69. A. N. Karkanis, P. N. Botsaris and P. D. Sparis, *Proc. Inst. Mech. Eng. Part D: J. Automob. Eng.*, **218**, 1333 (2004).
70. S.-C. Lee, J.-H. Jang, B.-Y. Lee, J.-H. Bae and S.-J. Choung, *Int. J. Automot. Technol.*, **5**, 1 (2004).
71. G. J. J. Bartley, *Top. Catal.*, **42–43**, 345 (2007).
72. M. Al-Hasan, *Am. J. Appl. Sci.*, **4**, 106 (2007).
73. D. D. Beck, J. W. Sommers and D. L. DiMaggio, *Appl. Catal. B*, **11**, 257 (1997).
74. P. Bera, Ph. D. Thesis, Indian Institute of Science, Bangalore, India, 2002.
75. R. K. Herz, *Ind. Eng. Chem. Prod. Res. Dev.*, **20**, 451 (1981).
76. R. K. Herz, J. B. Klela and J. A. Sell, *Ind. Eng. Chem. Prod. Res. Dev.*, **22**, 387 (1983).
77. K. M. Adams and H. S. Gandhi, *Ind. Eng. Chem. Prod. Res. Dev.*, **22**, 207 (1983).
78. R. Rainer, M. Koranne, S. M. Vesecky and D. W. Goodman, *J. Phys. Chem. B*, **101**, 10769 (1997).
79. R. Burch, *Pure Appl. Chem.*, **68**, 377 (1996).
80. J. H. Visser and R. E. Soltis, *IEEE Trans. Instrum. Meas.*, **50**, 1543 (2001).
81. H. C. Yao and Y. F. Yu Yao, *J. Catal.*, **86**, 254 (1984).
82. A. Trovarelli, *Comments Inorg. Chem.*, **20**, 263 (1999).
83. R. Di Monte and J. Kašpar, *Top. Catal.*, **28**, 47 (2004).
84. N. Kakuta, H. Ohkita and T. Mizushima, *J. Rare Earths*, **22**, 1 (2004).
85. Y.-F. Chang and J. G. McCarty, *Catal. Today*, **30**, 163 (1996).
86. X. Jiang, R. Zhou, J. Yuan, G. Lu and X. Zheng, *J. Rare Earths*, **21**, 55 (2003).
87. Y. Sakamoto, K. Kizaki, T. Motohiro, Y. Yokota, H. Sobukawa, M. Uenishi, H. Tanaka and M. Sugiura, *J. Catal.*, **211**, 157 (2002).
88. S. Bernal, G. Blanco, F. J. Botana, G. M. Gatica, J. A. Pérez Omil, J. M. Pintado, J. M. Rodríguez-Izquierdo, *J. Alloys Compd.* **207-208**, 196 (1994).
89. S. Otsuka-Yao-Matsuo, N. Izu, T. Omata and K. Ikeda, *J. Electrochem. Soc.*, **145**, 1406 (1998).
90. S. E. Golunski, H. A. Hatcher, R. R. Rajaram and T. Truex, *Appl. Catal. B*, **5**, 367 (1995).
91. H. Idriss and M. A. Barteau, *Adv. Catal.*, **45**, 261 (2000).
92. A. Troveralli, *Catal. Rev. Sci. Eng.*, **38**, 439 (1996).
93. A. Troveralli, in *Catalysis by Ceria and Related Materials*, Imperial College Press, London, 2002.
94. R. J. Gorte, *AIChE J.*, **56**, 1126 (2010).
95. C. Howitt, V. Pitchon and G. Maire, *J. Catal.*, **154**, 47 (1995).
96. J. Kašpar, P. Fornasiero and M. Graziani, *Catal. Today*, **50**, 285 (1999).
97. K. C. Taylor, *Catal. Rev. Sci. Eng.*, **35**, 457 (1993).
98. A. Martínez-Arias, R. Cataluña, J. C. Conesa and J. Soria, *J. Phys. Chem. B*, **102**, 809 (1998).
99. Lj. Kundakovic and M. Flytzani-Stephanopoulos, *Appl. Catal. A*, **171**, 13 (1998).
100. T. Murota, T. Hasegawa, S. Aozasa, H. Matsui and M. Motoyama, *J. Alloys Compd.*, **193**, 298 (1993).
101. P. Fornasiero, E. Fonda, R. Di Monte, G. Vlaic, J. Kašpar and M. Graziani, *J. Catal.*, **187**, 177 (1999).
102. R. Di Monte and J. Kašpar, *J. Mater. Chem.*, **15**, 633 (2005).
103. T. Baidya, Ph. D. Thesis, Indian Institute of Science, Bangalore, India, 2007.
104. S. Roy, Ph. D. Thesis, Indian Institute of Science, Bangalore,

India, 2007.

105. P. Bera, K. C. Patil, V. Jayaram, G. N. Subbanna and M. S. Hegde, *J. Catal.*, **196**, 293 (2000).

106. K. C. Patil, M. S. Hegde, T. Rattan and S. T. Aruna, in *Chemistry of Nanocrystalline Oxide Materials*, World Scientific, Singapore, 2008.

107. K. R. Priolkar, P. Bera, P. R. Sarode, M. S. Hegde, S. Emura, R. Kumashiro and N. P. Lalla, *Chem. Mater.*, **14**, 2120 (2002).

108. A. Gayen, K. R. Priolkar, P. R. Sarode, V. Jayaram, M. S. Hegde, G. N. Subbanna and S. Emura, *Chem. Mater.*, **16**, 2317 (2004).

109. P. Bera, A. Gayen, M. S. Hegde, N. P. Lalla, L. Spadaro, F. Frusteri and F. Arena, *J. Phys. Chem. B*, **107**, 6122 (2003).

110. P. Bera, K. R. Priolkar, A. Gayen, P. R. Sarode, M. S. Hegde, S. Emura, R. Kumashiro, V. Jayaram and G. N. Subbanna, *Chem. Mater.*, **15**, 2049 (2003).

111. P. Singh and M. S. Hegde, *Chem. Mater.*, **21**, 3337 (2009).

112. P. Bera, K. R. Priolkar, P. R. Sarode, M. S. Hegde, S. Emura, R. Kumashiro and N. P. Lalla, *Chem. Mater.*, **14**, 3591 (2002).

113. P. Bera, K. C. Patil and M. S. Hegde, *Phys. Chem. Chem. Phys.*, **2**, 3715 (2000).

114. P. Bera and M. S. Hegde, *Catal. Lett.*, **79**, 75 (2002).

115. G. Dutta, U. V. Waghmare, T. Baidya, M. S. Hegde, K. R. Priolkar and P. R. Sarode, *Chem. Mater.*, **18**, 3249 (2006).

116. G. Dutta, U. V. Waghmare, T. Baidya, M. S. Hegde, K. R. Priolkar and P. R. Sarode, *Catal. Lett.*, **108**, 165 (2006).

117. T. Baidya, A. Gayen, M. S. Hegde, N. Ravishankar and L. Dupont, *J. Phys. Chem. B*, **110**, 5262 (2006).

118. T. Baidya, A. Marimuthu, M. S. Hegde, N. Ravishankar and G. Madras, *J. Phys. Chem. C*, **111**, 830 (2007).

119. S. Roy, M. S. Hegde, N. Ravishankar and G. Madras, *J. Phys. Chem. C*, **111**, 8153 (2007).

120. S. Roy, M. S. Hegde, S. Sharma, N. P. Lalla, A. Marimuthu and G. Madras, *Appl. Catal. B*, **84**, 341 (2008).

121. P. Bera, K. C. Patil, V. Jayaram, M. S. Hegde and G. N. Subbanna, *J. Mater. Chem.*, **9**, 1801 (1999).

122. A. Gupta, M. S. Hegde, K. R. Priolkar, U. V. Waghmare, P. R. Sarode and S. Emura, *Chem. Mater.*, **21**, 5836 (2009).

123. T. Baidya, G. Dutta, M. S. Hegde and U. V. Waghmare, *Dalton Trans.*, 455 (2009).

124. T. Baidya, A. Gupta, P. A. Deshpandey, G. Madras and M. S. Hegde, *J. Phys. Chem. C*, **113**, 4059 (2009).

125. A. Gupta, A. Kumar, U. V. Waghmare and M. S. Hegde, *Chem. Mater.*, **21**, 4880 (2009).

126. P. Singh, M. S. Hegde and J. Gopalakrishnan, *Chem. Mater.*, **20**, 7268 (2008).

127. N. W. Cant, P. C. Hicks and B. S. Lennon, *J. Catal.*, **54**, 372 (1978).

128. Y.-F. Yu Yao, *J. Catal.*, **87**, 152 (1984).

129. S. H. Oh and C. C. Eickel, *J. Catal.*, **112**, 543 (1988).

130. E. Bekyarova, P. Fornasiero, J. Kašpar and M. Graziani, *Catal. Today*, **45**, 179 (1998).

131. A. M. Venezia, L. F. Liotta, G. Pantaleo, V. L. Parola, G. Deganello, A. Beck, Zs. Koppány, K. Frey, D. Horváth and L. Guczi, *Appl. Catal. A*, **251**, 359 (2003).

132. S. Roy, A. Marimuthu, M. S. Hegde and G. Madras, *Appl. Catal. B*, **71**, 23 (2007).

133. S. Roy and M. S. Hegde, *Catal. Commun.*, **9**, 811 (2008).

134. S. Roy, A. Marimuthu, M. S. Hegde and G. Madras, *Appl. Catal. B*, **73**, 300 (2007).

135. P. Granger, C. Dathy, J. J. Lecomte, L. Leclercq, M. Prignet, G. Mabilon and G. Leclercq, *J. Catal.*, **173**, 304 (1998).

136. P. Granger, J. J. Lecomte, C. Dathy, L. Leclercq and G. Leclercq, *J. Catal.*, **175**, 194 (1998).

137. P. Granger, L. Delannoy, J. J. Lecomte, C. Dathy, H. Praliaud, L. Leclercq and G. Leclercq, *J. Catal.*, **207**, 202 (2002).

138. J. H. Holles, M. A. Switzer and R. J. Davis, *J. Catal.*, **190**, 247 (2000).

139. D. R. Rainer, S. M. Vesecky, M. Koranne, W. S. Oh and D. W. Goodman, *J. Catal.*, **167**, 234 (1997).

140. M. Schmal, M. A. S. Baldaza and M. A. Vannice, *J. Catal.*, **185**, 138 (1999).

141. S. Roy, A. Marimuthu, M. S. Hegde and G. Madras, *Catal. Commun.*, **9**, 101 (2008).

142. S. Roy, B. Viswanath, M. S. Hegde and G. Madras, *J. Phys. Chem. C*, **112**, 6002 (2008).

143. S. Roy, A. Marimuthu, P. A. Deshpande, M. S. Hegde and G. Madras, *Ind. Eng. Chem. Res.*, **47**, 9240 (2008).

144. P. Avila, M. Montes and E. E. Miró, *Chem. Eng. J.*, **109**, 11 (2005).

145. V. Tomašić and F. Jović, *Appl. Catal. A*, **311**, 112 (2006).

146. V. Tomaši, *Catal. Today*, **119**, 106 (2007).

147. T. A. Nijhuis, A. E. W. Beers, T. Vergunst, I. Hoek, F. Kapteijn and J. A. Moulijn, *Catal. Rev. Sci. Eng.*, **43**, 345 (2001).

148. P. Jiang, G. Lu, Y. Guo, Y. Guo, S. Zhang and X. Wang, *Surf. Coat. Technol.*, **190**, 314 (2005).

149. S. Sharma and M. S. Hegde, *Catal. Lett.*, **112**, 69 (2006).

150. S. Sharma, M. S. Hegde, R. N. Das and M. Pandey, *Appl. Catal. A*, **337**, 130 (2008).

Parthasarathi Bera is a native of Moyna in Purba Medinipur district of West Bengal, India. He obtained his B. Sc. and M. Sc. in Chemistry from Jadavpur University, Kolkata and earned his Ph. D. in Heterogeneous Catalysis from Indian Institute of Science, Bangalore under the supervision of Professor M. S. Hegde. He worked as a Post Doctoral Fellow at University of Washington, Seattle, USA with Professor Charles T. Campbell and University of Pennsylvania, Philadelphia, USA with Professor John M. Vohs. He was a Marie Curie Fellow at Instituto de Catálisis y Petroleoquímica, CSIC, Madrid, Spain under Professor Arturo Martínez-Arias. He joined National Aerospace Laboratories, Bangalore as a Scientist Fellow in January 2010. His main research interests include heterogeneous catalysis for green energy and environment, materials chemistry and surface science and engineering.

M. S. Hegde received his Ph.D. from Indian Institute of Technology, Kanpur in 1976 and joined the Indian Institute of Science in 1977. He is a professor in Solid State and Structural Chemistry Unit and Dean of Science. His research interests are in the areas of surface science, solid state chemistry and catalysis.